QUANTIFYING THE EFFECT OF DISEASE CHARACTERISTICS ON THE OUTCOMES OF INTERVENTIONS USING MATHEMATICAL MODELLING

CASSANDRA LISITZA

A THESIS SUBMITTED TO THE FACULTY OF GRADUATE STUDIES
IN PARTIAL FULFILMENT OF THE REQUIREMENTS
FOR THE DEGREE OF
MASTER OF SCIENCE

GRADUATE PROGRAM IN DEPARTMENT OF MATHEMATICS AND STATISTICS
YORK UNIVERSITY
TORONTO, ONTARIO

FEBRUARY 2023

Abstract

Many emerging diseases have several common features in terms of their natural history; however, they differ in their quantifiable characteristics, such as transmissibility, the incubation period, and infectiousness profile. These characteristics are crucial in determining whether there will be a local outbreak of the disease or if it has the potential to evolve into a global pandemic. Understanding these characteristics and how they differ among diseases is thus critical in devising public health policies to prevent the spread of infection in the population and mitigate the evident repercussions that can result from a novel disease such as what was observed during the COVID-19 pandemic. This thesis delineates a general modelling framework for transmission dynamics of two respiratory infections, influenza and SARS-CoV-2, to investigate the effect their characteristics on intervention outcomes. Reflecting the novelty of the objectives in this thesis, the results indicate that increasing the severity of interventions (i.e., from isolation only, to school closure, to lockdown) leads to different outcomes for the two disease. Performing simulations and sensitivity analysis, we show that the length of infectious period, and infectiousness profile during various stages of illness have a remarkable influence on the outcome of interventions. Our findings indicate that the difference in school closure outcomes between SARS-CoV-2 and influenza may be due to longer and more infectious pre-symptomatic stage in the former disease compared to the latter. This is further demonstrated by the results from our sensitivity analysis, indicating that the pre-symptomatic and symptomatic periods consistently exhibit a negative linear correlation with the relative reduction in attack rate (i.e., the proportion of the population infectious throughout the outbreak), regardless of

the disease or the type of intervention.

To my grandparents...

Acknowledgements

First and foremost, thank you to my supervisor, Dr. Seyed Moghadas, for his immense help and guidance over the course of this research and for introducing me to this very exciting area of applied mathematics.

A special thanks to my colleagues in the ABM-Lab and the thesis committee members for providing their help and feedback throughout my MSc.

I would like to express my gratitude to my fiancé, Andrej Radonjić, for his constant support and always keeping me motivated.

Finally, I wish to thank my wonderful parents, Richard and Susan, as I could not have accomplished this endeavor without their constant love, encouragement, and support.

Contents

List of Tables

List of Figures

Chapter 1

Introduction

1.1 Modeling Infectious Diseases

Mathematical modeling has become an important approach in the field of epidemiology and public health, enabling researchers and policymakers to better understand the dynamical behavior of infectious diseases and the effect of control measures in a population. After the development of the Kermack-McKendrick classical epidemic model, this general framework was widely adapted in the twentieth century describing the interplay between susceptible (S), infected (I), and recovered (R) individuals in a population [1]. Kermack and McKendrick expressed that the level of susceptibility in a population must exceed a certain threshold for an epidemic to occur [1]. The susceptible-infected-recovered (SIR) is a fundamental framework still being used for studying infectious disease dynamics, including diseases such as influenza and Severe Acute Respiratory Syndrome (SARS), and COVID-19.

The general SIR model is a highly adept model that can be modified to offer important information on the spread of infectious disease, with a goal of advising public health policy to mitigate the effects of an epidemic [2]. It is common to include an exposed (E) class, representing individuals who are infected but not infectious yet, for infections such as influenza or COVID-19. More important is the possibility of an infected individual

becoming infectious without manifesting any signs (or symptoms) of the disease, often classified by terms of pre-symptomatic or asymptomatic infection. Individuals in these stages can transmit the disease before the onset of symptoms, or without ever developing any symptoms. In addition to evaluating the ability of a pathogen to spread within a population, epidemiological models are useful in assessing the effects of various control strategies and interventions [3]. The significance of epidemiological models was evident over the course of the COVID-19 pandemic. Control measures such as testing and isolation, school closures, lockdowns, and vaccination have been implemented, but understanding the degree to which such interventions contribute to the controllability of different infectious diseases with similar characteristics and natural history is still nascent. This thesis aims to improve this understanding using mathematical modelling.

1.2 Quantifiable Disease-Specific Characteristics

Many emerging diseases have several common features in terms of their natural history; however, they differ in their quantifiable characteristics, such as transmissibility (at different stages of disease; e.g., pre-symptomatic, symptomatic, and asymptomatic), the incubation period, and infectiousness profile [3]. These characteristics, being defined in Chapter 2, are crucial in determining whether there will be a local outbreak or if the disease has the potential to evolve into a global pandemic. Understanding these characteristics and how they differ among diseases is thus imperative in preventing the spread of infection in the population and mitigate the subsequent socioeconomic repercussions, which were evident during the COVID-19 pandemic.

Implementations of public health measures depend vitally on the aforementioned disease characteristics, which can determine the type and intensity of interventions, and their outcomes. For example, an intervention such as school closure has been proven effective in slowing the spread of the influenza virus [4, 5]; however, recent studies provide data-driven evidence that this intervention has largely been ineffective for blunting

community transmission of COVID-19 [6, 7]. This has been speculated to be due to the longer incubation period for SARS-CoV-2. Further, some diseases, such as Ebola, are only transmissible when the infected individual becomes severely ill after the onset of symptoms [8], while disease transmission can occur even prior to the onset of symptoms in several diseases like influenza, respiratory syncytial virus (RSV), and COVID-19. Understanding the degree to which such disease characteristics influence the effectiveness of interventions remains elusive.

1.3 Motivation

Despite the vast literature on disease modelling, the interplay between disease characteristics, infection dynamics, and the effectiveness of various interventions (e.g., lockdowns, school closure, social distancing, self-isolation, use of personal protective equipment (PPE), and vaccination) has not been fully investigated. Existing literature has largely evaluated the effect of interventions for a particular disease, without a systematic analysis of diseases with similar characteristics. Reflecting the novelty of this thesis, it is of utmost importance to evaluate why some intervention measures are effective in slowing the spread of particular diseases while being ineffective or less effective against others, and more specifically, how the characteristics of a disease affect intervention outcomes. The focus of this work will be on two major respiratory infections caused by SARS-CoV-2 and influenza to identify what interventions are most effective, and quantify their effectiveness in reducing the burden of disease based on similarities and differences in their epidemiological characteristics.

Chapter 2

Disease Characteristics and Interventions

2.1 Natural History

Diseases are characterized based on their natural history, which refers to the natural evolution/progression of a disease in an individual over time in the absence of treatment or other intervention. This progression starts from the time of exposure of a susceptible individual to the disease (and occurrence of infection), pathogenic changes occur in the individual and the disease is in the clinical or subclinical stages (Figure 2.1). Diseases with similar biology and epidemiology to Influenza (like COVID-19) may represent both states where a pre-symptomatic stage is followed by the symptomatic stage after the onset of symptoms, where most diagnosis takes place. During this stage, a number of outcomes are possible such as hospitalization (if the illness is severe or critical), death, or improvement towards recovery [9]. The amount of time spent in each stage is critical in determining if there will be an outbreak, and how interventions should be implemented. To further evaluate the risk of an outbreak, characteristics such as the transmissibility, incubation period, pre-symptomatic period, symptomatic period, and the ratio of asymptomatic to symptomatic cases are important epidemiological parameters [9]. Differences in these

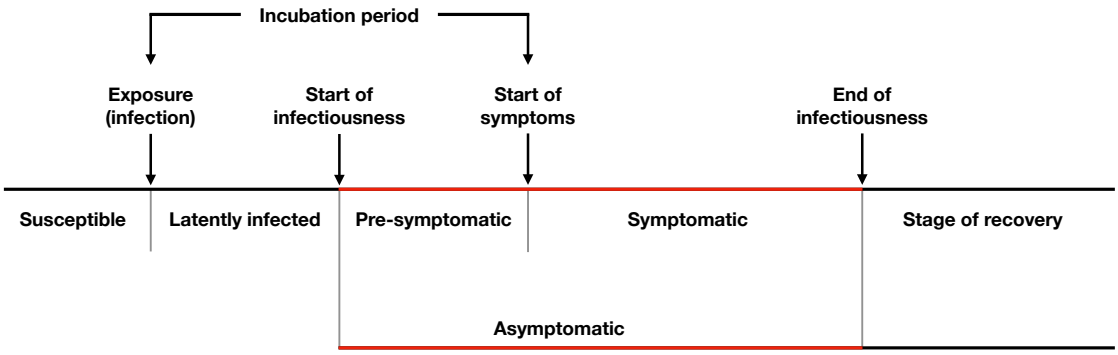

Figure 2.1: Natural history of a disease with similar characteristics to influenza and COVID-19.

parameters among different respiratory diseases would allow us to optimally implement interventions to mitigate the effects of a pandemic.

2.1.1 Infectiousness Profile

For majority of respiratory infections, there are mainly two different stages of disease in which individuals are infectious. First, there is asymptomatic infection, which occurs when an infected individual renders no symptoms. These individuals may be able to transmit the disease to other susceptible individuals [10]. For diseases such as influenza and COVID-19, many asymptomatic cases go unknown [10]. However, mass and random testing can often identify these cases similar to the scenario observed during the COVID-19 pandemic. Similar to asymptomatic infection is pre-symptomatic infection, which refers to the stage in which infection can be detected, but symptoms of the disease are not yet developed. The pre-symptomatic stage is often infectious and disease transmission can occur[11]. For a disease such as COVID-19, the number of asymptomatic cases greatly affects the pandemic potential and control in the population. Further, the length of the pre-symptomatic period in individuals also dictates the trajectory of an outbreak as well as the effect of interventions [12, 13]. A prolonged pre-symptomatic period makes the uncontrolled transmission more likely. Investigation of COVID-19 indicates that the pre-symptomatic stage is the most infectious stage of disease [14]. Combined with its longer duration compared to pre-symptomatic stage in influenza [2], the controllability of

COVID-19 appears more challenging [7].

Second, there is symptomatic infection, during which the individuals manifest symptoms of the disease and the likelihood of disease detection increases. In this case, testing with positive identification of disease can prompt immediate isolation after the onset of symptoms to minimize and potentially eliminate onward transmission of the pathogen [11].

The infectiousness profile of a given disease has a considerable impact on its spread in the population. Thus, it is important to consider these parameters in an effort to mitigate the burden of a disease. SARS-CoV-2 has a high infectiousness level immediately before the onset of symptoms, highlighting the necessity for early detection and isolation, or quarantine of individuals exposed to known cases of disease, as well as the use of personal protective equipment (such as masks) to limit transmission [15].

2.2 Influenza

Influenza is a viral disease with recorded existence of many centuries [16], but most documentation on influenza is from the last century. The first pandemic of the last century occurred during World War I in 1918 [17]. Influenza virus was thought to have killed nearly 200,000 Americans during the 1918 pandemic [18] and millions of people worldwide [19, 20]. Over the course of a century, there have been three additional influenza pandemics, including H1N1, H2N2, and H3N2 [21]. It was not until the influenza virus was isolated in a laboratory in the 1930s that a vaccine was developed [16]. Presently, seasonal influenza epidemics are common annually in most countries and outbreaks are widely unpredictable [16]. However, there are a few key trends that we perceive. Influenza epidemics are more likely to occur during colder months of any geographic region. Moreover, these epidemics occur largely due to viral mutations, referred to as antigenic drift and/or shift, escaping pre-existing immunity. This necessitates the generation of new vaccines every year based on the expected virus to spread [16, 21]. Influenza viruses cause significant morbidity and

mortality, and pose great social and economic burden. Given that influenza viruses infects 20 to 40 percent of the population per annum, ongoing research is needed to reduce the associated risk factors and prevent excess mortality [21].

Although vaccines become available prior to the start of annual seasonal epidemics, vaccination coverage is suboptimal, especially among younger age groups who have lower risk of severe outcomes, but contribute to disease transmission more significantly compared to older adults.. Epidemiological studies suggest that with a lack of avoidance behaviour, including monitoring contacts and social distancing, influenza can spread and evolve into an epidemic even in vaccinated populations [22].

2.2.1 Influenza Types

There are four types of influenza virus: influenza A, B, C, and D [16]. Of these, influenza A and B cause infections during seasonal influenza, and influenza A is the only type known to have caused pandemics in the human population. The main source of influenza epidemics in human history is from the H1N1, H2N2, and H3N2 strains, which are subtypes of influenza A. Another type, although not common, is the Avian flu which has led to infections, hospitalizations, and death in humans. Influenza A subtypes induce symptoms such as fever, chills, achiness, drowsiness, sneezing, coughing, and sore throat [23].

2.3 SARS-CoV-2

In late 2019, SARS-CoV-2 caused a local outbreak in Wuhan, China, that within a few weeks resulted in a global pandemic, known as COVID-19 [23]. SARS-CoV-2, like influenza, is a contagious respiratory illness with similar symptoms. However, SARS-CoV-2 has been estimated to be significantly more transmissible than influenza. A distinguishable feature of SARS-CoV-2 is the lengthy incubation period in comparison to that of other diseases, such as influenza or ebola virus [7]. Recent studies have shown that

COVID-19 is highly infectious before symptom onset [15], and it was found that most transmissions occur as a result of contacts with individuals who are infectious, but do not manifest symptoms [2, 15].

2.3.1 Variants of SARS-CoV-2

SARS-CoV-2 can mutate and generate new variants that may be more transmissible or cause more severe disease. In the context of SARS-CoV-2, the World Health Organization (WHO) defined both a variant of concern (VOC) and variant of interest (VOI) [24]. A VOC is defined as a variant which has increased transmissibility with an increased number of resulting fatalities and a decrease in vaccine effectiveness. A VOI is thought to affect factors such as transmissibility, disease severity, immune escape, and diagnostics [23, 24].

Over the course of COVID-19 pandemic, a number of VOCs have emerged in different geographic locations, and spread worldwide. For instance, the Alpha variant (B.1.1.7), was first identified in the United Kingdom in September 2020 and reached Canada by April 2021. Its transmissibility was estimated to be 50% greater than that of the original wild-type Wuhan-I virus [25, 26]. By June 2021, Alpha was responsible for more than 50% of recorded SARS-CoV-2 cases in Canada [23].

Following Alpha, the Delta variant (B.1.617.2) emerged, initially detected in India in October 2020 during a period of low vaccine coverage [27]. Naturally, the emergence of this highly invasive variant resulted in significant hospitalizations and deaths, with an estimated 30% increase in transmissibility compared to the Alpha variant [28, 29]. The final VOC considered in this thesis, and the most transmissible variant, was Omicron, which was estimated to be 35% more than transmissible than the Delta variant [30].

In addition to the VOC variants, a number of VOI variants emerged during the COVID-19. For example, the Beta variant (B.1.351) was first identified in South Africa in May of 2020 with an increased transmissibility compared to the original Wuhan-I virus. Although the Beta variant also resulted in hospitalizations and deaths, these outcomes were not nearly as significant as those occurred during infection waves of the Alpha and Delta

variants [23]. Another VOI is the gamma variant (P.1) that was first reported in Brazil in November of 2020. Although it was estimated to be 1.7-2.4 times more transmissible than the original strain of SARS-COV-2 [31], the gamma variant did not become as prevalent as the Alpha or Delta variants [23].

2.4 Non-Pharmaceutical Interventions

The primary goal of public health, in the event of an epidemic, is to prevent disease spread in the population, and mitigate severe outcomes such as hospitalization and death. In recent studies, it was found that over the course of the COVID-19 pandemic, the implementation of public health policies including the use of masks and other PPE, social distancing, quarantine and isolation, school and workplace closures, and lockdown proved effective, albeit in varying degrees, in preventing the spread of COVID-19 [4]. In this thesis, we focus on the three key non-pharmaceutical measures outlined below.

2.4.1 Quarantine and Isolation

A common means of reducing disease spread is quarantine, which is recommended for individuals who have had contact(s) with known infectious cases. Isolation is another measure that is recommended for individuals who are identified to be infected with, or show symptoms of the disease. Recent studies indicate that it is critical for infected individuals to quarantine or self-isolate to prevent onward transmission [32–34].

2.4.2 School Closure

Given that school children aged 5–18 are highly socially active with other individuals in the same age group and family members, school closures are often considered an important measure to decrease contact and mitigate disease transmission.

2.4.3 Lockdown

A lockdown is a much stricter intervention measure, which includes both isolation, closure of schools and businesses, and may restrict movements of individuals and direct contacts. This intervention was implemented in many affected countries during the early stages of COVID-19 pandemic [35–37].

Chapter 3

Epidemiological Parameters: Influenza and SARS-CoV-2 Variants

There are five key characteristics that significantly affect the dynamical behavior of disease spread in a population [3]. We often discuss infectious disease dynamics in terms of their transmissibility, incubation period, pre-symptomatic period, symptomatic period, and ratio of asymptomatic to symptomatic cases. Mathematically, transmission of any respiratory disease can be characterized by the basic reproduction number (R_0), defined as the average number of new infections caused by an infectious individual in a totally susceptible population [3]. Essentially, this number measures the potential for a disease to spread through a population. The incubation period of a disease refers to the period between the time of infection and the onset of symptoms. The pre-symptomatic period of a disease is the time-interval between the start of infectiousness and the onset of symptoms in an infected individual. The symptomatic period refers to an infectious period during which symptoms are present. In a modelling context, often the symptomatic period and infectious period are used interchangeably after the onset of symptoms. However, in a clinical context, there are two distinct concepts, possibly representing two different durations. Here, we consider the infectious period after the onset of symptoms. Finally, the proportion of infected individuals that develop symptomatic disease varies across

Table 3.1: Estimates of the epidemiological parameters of influenza A/H1N1.

Influenza A/H1N1		
Characteristic	**Estimate**	**Reference**
Reproduction number	1.27	[38]
Incubation period	$1-2$ days	[39, 40]
Pre-symptomatic period	$0-1$ days	[41]
Infectious period	$4-7$ days	[42]
Asymptomatic proportion of infections	$4-28\%$, $33-50\%$, 44%	[43–45]

different diseases.

3.1 Influenza

3.1.1 H1N1

One of the most common strains of influenza A that spread through the human population is H1N1, with an estimated reproduction number between 1.2–1.8 [22, 38]. For the incubation period, a consistent mean of $1-2$ days has been reported [39, 40]. The pre-symptomatic period for H1N1 has a range of $0-1$ days [41]. The symptomatic period varies from $4-7$ days [42]. The ratio of asymptomatic for the H1N1 strain has been estimated to vary between $4-50\%$ [43–45]. Estimates of these parameters are provided in Table 3.1.

3.2 SARS-CoV-2

3.2.1 Original Wuhan-I Strain

In comparison to H1N1, SARS-CoV-2 is more transmissible. The original strain was estimated to have a reproduction number in the range $2-3.5$ [46]. Further, SARS-CoV-2

Table 3.2: Estimates of the epidemiological parameters of the original SARS-CoV-2 strain.

SARS–CoV-2: Original strain		
Characteristic	**Estimate**	**Reference**
Reproduction number	3.36	[30]
Incubation period	5.2 days	[47, 48]
Pre-symptomatic period	2.3 days	[2, 47]
Infectious period	3.2 days	[2, 47]
Asymptomatic proportion of infections	30.8%, 35.1%	[49, 50]

original strain was found to have a longer incubation period than H1N1, with a mean of 5.2 days [47, 48]. The pre-symptomatic period and infectious periods after the onset of symptoms also differed from those of H1N1, with the mean of 2.3 days and 3.2 days, respectively [2, 47]. The proportion infections being asymptomatic ranged between 30% to 35.1% [49, 50].

3.2.2 Alpha Variant

The Alpha variant was more transmissible than the original strain, with a reproduction number of 4.8 [51]. The incubation period of the Alpha variant was estimated to be 5.0 days [52]. The pre-symptomatic period had the mean in the range $3.94 - 4.65$ days [53]. The infectious period of the Alpha variant was estimated to be 5.1 days on average [54]. Finally, the proportion of infections being asymptomatic was approximately 16.7% [55].

3.2.3 Delta Variant

The Delta variant was even more transmissible than the Alpha variant, with reproduction numbers of 5.37 and 5.94 [51, 57]. Furthermore, the Delta variant had an incubation period of 4.41 days [52]. The pre-symptomatic period of this variant varied in the range $3.49 - 3.93$ days [53]. After the onset of symptoms, the infectious period may be up to 8.89 days [58]. The proportion of infections being asymptomatic was found to be between

Table 3.3: Estimates of the epidemiological parameters of the the SARS-CoV-2 Alpha variant

SARS–CoV-2: Alpha variant		
Characteristic	**Estimate**	**Reference**
Reproduction number	4.8	[51]
Incubation period	5 days	[52]
Pre-symptomatic period	$3.94 - 4.65$ days	[53]
	$1 - 4$ days	[56]
Infectious period	5.1 days	[54]
Asymptomatic proportion of infections	16.7%	[55]

8.4% and 13.7% among all age groups [59, 60].

3.2.4 Omicron Variant

The most transmissible variant (at the time of this thesis) was Omicron, with a reproduction number of 9.5 [62]. The incubation period is the shortest among all variants, with an average of 3.41 days [52]. The pre-symptomatic period of the Omicron variant is approximately 2 days [63]. The infectious period for this variant is estimated to be 6.87

Table 3.4: Estimates of the epidemiological parameters of the the SARS-CoV-2 Delta variant

SARS–CoV-2: Delta variant		
Characteristic	**Estimate**	**Reference**
Reproduction number	5.94	[51]
	5.37	[57]
Incubation period	4.41 days	[52]
Pre-symptomatic period	$3.49 - 3.93$ days	[53]
	2 days	[61]
Infectious period	8.89 days	[58]
Asymptomatic proportion of infections	8.4%, 13.7%	[59, 60]

Table 3.5: Estimates of the epidemiological parameters of the the SARS-CoV-2 Omicron variant

SARS–CoV-2: Omicron variant		
Characteristic	**Estimate**	**Reference**
Reproduction number	9.5	[62]
Incubation period	3.41 days	[52]
	3.33 days	[65]
Pre-symptomatic period	2 days	[63]
Infectious period	6.87 days	[58]
Asymptomatic proportion of infections	32.4%	[64]

days [58]. Finally, the proportion of infections being asymptomatic is estimated around 32.4% [64].

Chapter 4

General Modelling Framework

This chapter provides details of the model structure used to quantify the effect of interventions for influenza A/H1N1 and SARS-CoV-2 variants. We discuss an age-structured model with the inclusion of contact patterns, and how interventions are implemented using contact matrices. Age structure was incorporated in the model because of its importance in the population dynamics for the spread of infection. We introduce an extended version of the susceptible-exposed-infectious-recovered (SEIR) compartmental model with added compartments to differentiate the infectiousness at various stages of the disease, isolation of infectious individuals, and waning immunity. In addition to deriving the reproduction number of the model analytically, we simulate the deterministic model where key parameters were sampled from their respective distributions. A sensitivity analysis was performed using partial rank correlation coefficients (PRCC) to determine the relative importance of each parameter in determining the effectiveness of interventions.

4.1 The Model

The model incorporated several age groups to capture the effects of contact patterns related to school closure, isolation, and lockdown interventions. The age groups considered in the model are 0–4, 5–18, 19–49, 50–64, and 65+ years old. Compartments for asymptomatic

and pre-symptomatic stages are also included, given their importance in the natural history of infection for both influenza and SARS-CoV-2. Since reinfection may occur in these respiratory diseases, waning immunity is included in the general framework. Finally, since individuals can be reinfected, an additional exposed class is included to capture the decreased level of susceptibility of those who have been previously infected, and are less likely to become symptomatic due to pre-existing immune responses.

Using the variables described in Table 4.1, the dynamics of disease spread and control can be expressed by the following system of differential equations:

$$\begin{aligned}
S_a' &= -S_a \mathscr{J}_a \\
E_a' &= S_a \mathscr{J}_a - \sigma E_a \\
A_a' &= p\sigma E_a + p_r \sigma E_{r,a} - \gamma_A A_a \\
P_a' &= (1-p)\sigma E_a + (1-p_r)\sigma E_{r,a} - \theta P_a \\
I_a' &= (1-q)\theta P_a - \gamma I_a \\
Q_a' &= q\theta P_a - \gamma Q_a \\
R_a' &= \gamma_A A_a + \gamma Q_a + \gamma I_a - \nu R_a \\
W_a' &= \nu R_a - W_a \mathscr{J} \\
E_{r,a} &= W_a \mathscr{J} - \sigma E_{r,a}
\end{aligned} \tag{4.1}$$

where $\mathscr{J}_a$ describes the force of infection, and is defined by the following equation

$$\mathscr{J}_a = \beta \sum_{j=1}^{5} M_a^R \left(\frac{\alpha A_j + \zeta P_j + \kappa I_j}{N_j} \right) + \beta \sum_{j=1}^{5} M_a^I \left(\frac{\kappa Q_j}{N_j} \right),$$

The parameter β represents the transmission rate, M_j^R is the matrix describing regular contact patterns of age group j with any other age group, M_j^I is the matrix describing contact patterns of isolated individuals in age group j with any other age group, and N_j is

Table 4.1: Description of the model variables.

Variable	Description
S_a	Susceptible individuals in age group a
E_a	Exposed (and infected) individuals in age group a
A_a	Asymptomatic individuals in age group a
P_a	Pre-symptomatic individuals in age group a
I_a	Symptomatic individuals in age group a
Q_a	Isolated symptomatic individuals in age group a
R_a	Recovered individuals in age group a
W_a	Individuals in age group a whose immunity has waned
$E_{r,a}$	Re-exposed (and reinfected) individuals in age group a

the total number of individuals in age group j, given by:

$$N_j = S_j + E_j + A_j + P_j + I_j + Q_j + R_j + W_j + E_{r,j}$$

The force of infection describes how a susceptible individual in age group a will become infected through contacts with either asymptomatically, pre-symptomatically, or symptomatically infected individuals. Naturally, these individuals go through the exposed stage first with a an average duration of $1/\sigma$. A proportion p of the infected individuals will become asymptomatic and the remaining proportion proceeds to the pre-symptomatic stage. After an average duration of $1/\theta$, pre-symptomatic individuals will develop symptoms, and a proportion q of them will be identified and isolated. All infected individuals, whether asymptomatic or symptomatic, recover after an average infectious periods of $1/\gamma_A$ and $1/\gamma$, respectively. We assume that isolation of symptomatic individuals starts immediately following the onset of symptoms. Recovered individuals lose their immunity over time. We represent the average duration of protection in recovered individuals with $1/\nu$. Loss of immunity may result in re-infection. Reinfected individuals will follow a similar natural history as those primary infected individuals, but a proportion

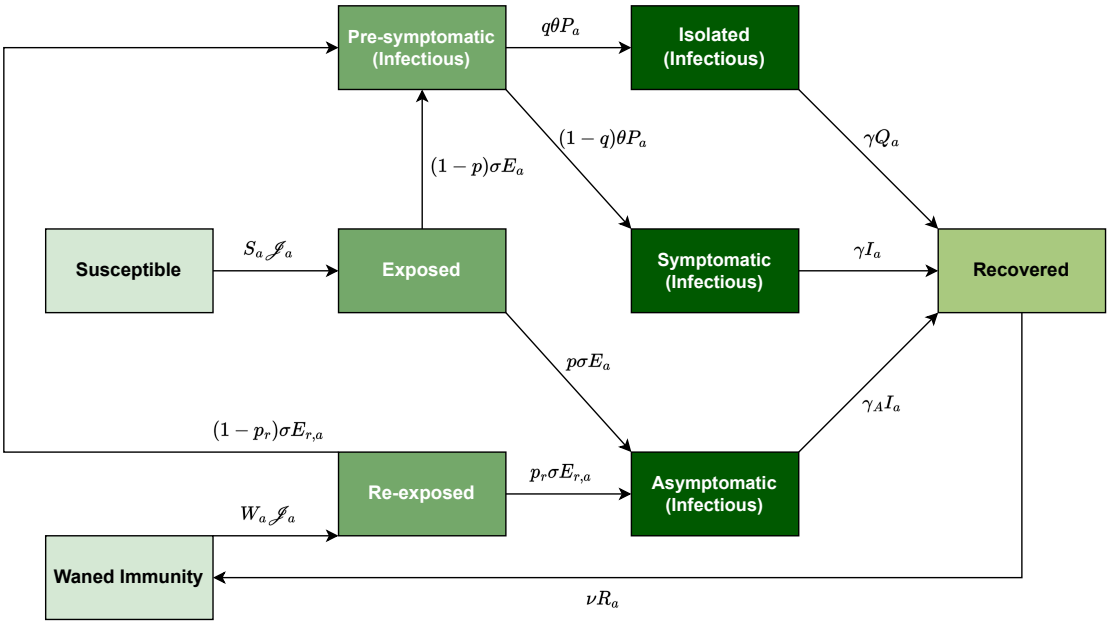

Figure 4.1: Schematic diagram depicting the general model dynamics represented in (4.1.)

p_r of whom may develop symptoms. Due to the effect of pre-existing immunity, the proportion p_r may be different from the proportion p assumed for the primary infected individuals. The dynamics of model is schematically represented in Figure 4.1. In this thesis, the focus will be on the model outcomes in the absence of waning immunity or re-infection.

4.1.1 Modelling with Interventions

Compartments can be added to the general model (4.1) to capture the effects of implementing an intervention, such as isolation. For interventions such as school closures and lockdowns, the effect is captured using the contact patterns observed and are represented in contact matrices. For the general model, isolation is the only intervention. Note that a lockdown includes both isolation and school closures. For the baseline scenario, regular contact patterns in the population were assumed. Further to the baseline scenario, we considered three scenarios with different intervention strategies, assuming that isolation is part of all these scenarios.

4.1.2 Baseline with Regular Contact Patterns (S1)

With regular contact patterns in the population and no individuals self-isolation, the force of infection is described as follows

$$\mathscr{J}_a^B = \beta \sum_{j=1}^{5} M_a^R \left(\frac{\alpha A_j + \zeta P_j + \kappa I_j}{N_j} \right)$$

where M_a^R represents the contact matrix for regular, normal sociala activities.

4.1.3 Regular Contact Patterns with Isolation (S2)

This corresponds to the general framework described before with the force of infection defined by

$$\mathscr{J}_a^B = \beta \sum_{j=1}^{5} M_a^R \left(\frac{\alpha A_j + \zeta P_j + \kappa I_j}{N_j} \right) + \beta \sum_{j=1}^{5} M_a^I \left(\frac{\kappa Q_j}{N_j} \right),$$

where M_a^R and M_a^I represent contact matrices for non-isolated and isolated individuals, respectively.

4.1.4 School Closure (S3)

We assume that school closure is implemented for the age group 5–18. In this intervention, other age groups have their regular contacts. The force of infection is then described by the equation

$$\begin{aligned}\mathscr{J}_a^S = \beta \sum_{j=1,3,4,5} M_a^R \left(\frac{\alpha A_j + \zeta P_j + \kappa I_j}{N_j} \right) + \beta \sum_{j=1}^{5} M_a^I \left(\frac{\kappa Q_j}{N_j} \right) \\ + \beta \sum_{j=2} M_a^S \left(\frac{\alpha A_j + \zeta P_j + \kappa I_j}{N_j} \right)\end{aligned}$$

where M_a^R, M_a^I, and M_a^S represent contact matrices for non-isolated, isolated individuals, and school children age group, respectively.

4.1.5 Lockdown (S4)

The lockdown intervention includes both isolation and school closure. The force of infection is defined by

$$\mathscr{J}_a^L = \beta \sum_{j=1}^{5} M_a^L \left(\frac{\alpha A_j + \zeta P_j + \kappa I_j}{N_j} \right) + \beta \sum_{j=1}^{5} M_a^I \left(\frac{\kappa Q_j}{N_j} \right)$$

where M_a^L and M_a^I represent contact matrices for non-isolated, and isolated individuals, respectively under the lockdown intervention.

4.1.6 Contact Patterns

Contact matrices were derived using data from the period of time (2018–2019) before and during (2020-2021) the early stages of COVID-19 pandemic in the province of Quebec [66]. These matrices were obtained based on a survey of $1,291$ Quebecers participating in both time periods. The assumption was that a contact is defined as a two-way conversation at a distance of less than 2 meters apart and without the use of a mask or other PPE. Poisson distributed, weighted generalized linear regression models were used to compare the mean number of social contacts over time, characterized by socio-demographic factors documented in the surveys [66]. The resulting matrices represent the average number of daily contacts of an individual in a specific age group with individuals in any other age groups. The matrices corresponding to interventions are:

1. Regular contacts

$$M^R = \begin{array}{c} \begin{matrix} 0-4 & 5-18 & 19-49 & 50-64 & 65+ \end{matrix} \\ \begin{bmatrix} 2.45 & 1.84 & 4.29 & 1.12 & 0.51 \\ 0.34 & 9.89 & 4.69 & 1.34 & 0.50 \\ 0.41 & 2.21 & 8.55 & 1.93 & 0.69 \\ 0.23 & 1.24 & 5.40 & 3.04 & 1.35 \\ 0.16 & 0.88 & 3.20 & 1.76 & 2.00 \end{bmatrix} \end{array} \begin{array}{l} \textbf{Age} \\ 0-4 \\ 5-18 \\ 19-49, \\ 50-64 \\ 65+ \end{array}$$

2. Contacts of isolated individuals

$$M^I = \begin{array}{c} \begin{matrix} 0-4 & 5-18 & 19-49 & 50-64 & 65+ \end{matrix} \\ \begin{bmatrix} 0.69 & 0.52 & 1.20 & 0.31 & 0.14 \\ 0.09 & 2.77 & 1.32 & 0.38 & 0.14 \\ 0.12 & 0.62 & 2.39 & 0.54 & 0.19 \\ 0.06 & 0.35 & 1.51 & 0.85 & 0.38 \\ 0.04 & 0.25 & 0.90 & 0.49 & 0.56 \end{bmatrix} \end{array} \begin{array}{l} \textbf{Age} \\ 0-4 \\ 5-18 \\ 19-49, \\ 50-64 \\ 65+ \end{array}$$

3. Contacts during school closure

$$M^S = \begin{array}{c} \begin{matrix} 0-4 & 5-18 & 19-49 & 50-64 & 65+ \end{matrix} \\ \begin{bmatrix} 2.45 & 1.84 & 4.29 & 1.12 & 0.51 \\ 0.34 & 3.80 & 4.69 & 1.34 & 0.50 \\ 0.41 & 2.21 & 8.55 & 1.93 & 0.69 \\ 0.23 & 1.24 & 5.40 & 3.04 & 1.35 \\ 0.16 & 0.88 & 3.20 & 1.76 & 2.00 \end{bmatrix} \end{array} \begin{array}{l} \textbf{Age} \\ 0-4 \\ 5-18 \\ 19-49, \\ 50-64 \\ 65+ \end{array}$$

4. Contacts during lockdown

$$M^L = \begin{array}{c} \begin{matrix} 0-4 & 5-18 & 19-49 & 50-64 & 65+ & \textbf{Age} \end{matrix} \\ \left[\begin{array}{ccccc|l} 1.74 & 0.78 & 1.99 & 0.63 & 0.19 & 0-4 \\ 0.31 & 4.10 & 2.88 & 0.70 & 0.31 & 5-18 \\ 0.51 & 1.92 & 6.60 & 1.83 & 0.87 & 19-49, \\ 0.34 & 1.03 & 3.94 & 2.41 & 1.52 & 50-64 \\ 0.06 & 0.23 & 0.98 & 0.80 & 1.63 & 65+ \end{array}\right] \end{array}$$

4.2 Model Parameterization

We assumed a population of $100,000$ individuals with an age distribution resembling the province of Ontario. The age distribution is 4.8% (0–4 years old), 16.4% (5–18 years old), 40.8% (19–49 years old), 20.4% (50–64 years old), and 17.6% (65+ years old). The general modelling framework assumes that

- Individuals who are isolated are infectious and can transmit the virus, but at a lower rate due to reduced contacts
- Asymptomatic individuals do not self-isolate, and assumed to follow their regular, normal social activities, unless lockdown intervention is implemented

We initiated simulations with 1 exposed individual in each age group. Thus, $S_a(0) = N_a - 1$. All other variables were initially set to 0. The initial values for different age groups are summarized in Table 4.2.

4.3 Derivation of the Basic Reproduction Number

The basic reproduction number (R_0) of the general model (4.1) can be derived theoretically using several different methods, including the Next Generation Matrix method or Fixed Point method [67, 68].

Table 4.2: Initial conditions for different age groups at the start of simulations.

Initial Conditions			
Age group	$\mathbf{N_a}$	$\mathbf{E_a(0)}$	$\mathbf{S_a(0)}$
0–4	4,800	1	4,799
5–18	16,400	1	16,399
19–49	40,800	1	40,799
50–64	20,400	1	20,399
65+	17,600	1	17,599
Total	100,000	5	995,000

In the absence of any interventions, the model reduces to the following system of differential equations:

$$\begin{aligned} S_a' &= -S_a \mathscr{J}_a, \\ E_a' &= S_a \mathscr{J}_a - \sigma E_a, \\ A_a' &= p\sigma E_a - \gamma_A A_a \\ P_a' &= (1-p)\sigma E_a - \theta P_a, \\ I_a' &= \theta P_a - \gamma I_a, \\ R_a' &= \gamma_A A_a + \gamma I_a, \end{aligned} \tag{4.2}$$

where the force of infection $\mathscr{J}_a$ is

$$\mathscr{J}_a = \beta \sum_{j=1}^{5} M_a^R \left(\frac{\alpha A_j + P_j + \kappa I_j}{N_j} \right)$$

We use the method presented by van den Driessche and Watmough, which implements a variation of the Next Generation Matrix method [69]. The five age groups can be grouped into n homogeneous compartments and separated based on whether they are infectious or non-infectious. Consider a vector $x = (x_1, ..., x_n)^t$ where $x_i \geq 0$ is the number of individuals in each compartment. The first m compartments are designated for the

infected individuals, which we clearly define based on the interpretation of our model. Let $X_s = \{x \geq 0 \mid x_i = 0,\ i = 1,...,m\}$ be the set of all disease-free states. To derive R_0 using this method, it is crucial to distinguish new infections among other changes in the population. Let $\mathscr{F}$ and $\mathscr{V}$ denote column vectors for the infected and uninfected components of our model, respectively. We consider any exposed, asymptomatic, pre-symptomatic, or symptomatic individual as our 'infected' population.

First, we linearize (4.2) at the disease-free equilibrium (DFE), $(S_a(0),0,0,...,0)$, to obtain

$$
\begin{aligned}
E_a' &= \beta S_a(0) \sum_{i=1}^{5} M_{a,i}^R \left(\frac{\alpha A_i + \zeta P_i + \kappa I_i}{N_i} \right) - \sigma E_a \\
A_a' &= p\sigma E_a - \gamma_A A_a \\
P_a' &= (1-p)\sigma E_a - \theta P_a \\
I_a' &= \theta P_a - \gamma I_a
\end{aligned}
$$

Then we defined the following matrix [69]:

$$
K_r = \begin{bmatrix}
\frac{M_{1,1}^R S_1(0)}{N_1} & \frac{M_{1,2}^R S_1(0)}{N_2} & \frac{M_{1,3}^R S_1(0)}{N_3} & \frac{M_{1,4}^R S_1(0)}{N_4} & \frac{M_{1,5}^R S_1(0)}{N_5} \\
\frac{M_{2,1}^R S_2(0)}{N_1} & \frac{M_{2,2}^R S_2(0)}{N_2} & \frac{M_{2,3}^R S_2(0)}{N_3} & \frac{M_{2,4}^R S_2(0)}{N_4} & \frac{M_{2,5}^R S_2(0)}{N_5} \\
\frac{M_{3,1}^R S_3(0)}{N_1} & \frac{M_{3,2}^R S_3(0)}{N_2} & \frac{M_{3,3}^R S_3(0)}{N_3} & \frac{M_{3,4}^R S_3(0)}{N_4} & \frac{M_{3,5}^R S_3(0)}{N_5} \\
\frac{M_{4,1}^R S_4(0)}{N_1} & \frac{M_{4,2}^R S_4(0)}{N_2} & \frac{M_{4,3}^R S_4(0)}{N_3} & \frac{M_{4,4}^R S_4(0)}{N_4} & \frac{M_{4,5}^R S_4(0)}{N_5} \\
\frac{M_{5,1}^R S_5(0)}{N_1} & \frac{M_{5,2}^R S_5(0)}{N_2} & \frac{M_{5,3}^R S_5(0)}{N_3} & \frac{M_{5,4}^R S_5(0)}{N_4} & \frac{M_{5,5}^R S_5(0)}{N_5}
\end{bmatrix}
$$

Thus, matrices $F_{20\times20}$ and $V_{20\times20}$ can be expressed by:

$$F_{20\times20} = \begin{array}{c} \\ E_a \\ A_a \\ P_a \\ I_a \end{array} \begin{array}{c} \begin{array}{cccc} E_a & A_a & P_a & I_a \end{array} \\ \begin{bmatrix} [0]_{5\times5} & \beta\alpha\,[K_r]_{5\times5} & \beta\zeta\,[K_r]_{5\times5} & \beta\kappa\,[K_r]_{5\times5} \\ [0]_{5\times5} & [0]_{5\times5} & [0]_{5\times5} & [0]_{5\times5} \\ [0]_{5\times5} & [0]_{5\times5} & [0]_{5\times5} & [0]_{5\times5} \\ [0]_{5\times5} & [0]_{5\times5} & [0]_{5\times5} & [0]_{5\times5} \end{bmatrix} \end{array}$$

and

$$V_{20\times20} = \begin{array}{c} \\ E_a \\ A_a \\ P_a \\ I_a \end{array} \begin{array}{c} \begin{array}{cccc} E_a & A_a & P_a & I_a \end{array} \\ \begin{bmatrix} \sigma[I]_{5\times5} & [0]_{5\times5} & [0]_{5\times5} & [0]_{5\times5} \\ -p\sigma[I]_{5\times5} & \gamma_A[I]_{5\times5} & [0]_{5\times5} & [0]_{5\times5} \\ -(1-p)\sigma[I]_{5\times5} & [0]_{5\times5} & \theta[I]_{5\times5} & [0]_{5\times5} \\ [0]_{5\times5} & [0]_{5\times5} & -\theta[I]_{5\times5} & \gamma[I]_{5\times5} \end{bmatrix} \end{array}$$

for $a = 1,\ 2,\ 3,\ 4,\ 5$, which gives

$$V^{-1}_{20\times20} = \begin{array}{c} \\ E_a \\ A_a \\ P_a \\ I_a \end{array} \begin{array}{c} \begin{array}{cccc} E_a & A_a & P_a & I_a \end{array} \\ \begin{bmatrix} \frac{1}{\sigma}[I]_{5\times5} & [0]_{5\times5} & [0]_{5\times5} & [0]_{5\times5} \\ \frac{p}{\gamma_A}[I]_{5\times5} & \frac{1}{\gamma_A}[I]_{5\times5} & [0]_{5\times5} & [0]_{5\times5} \\ \frac{(1-p)}{\theta}\sigma[I]_{5\times5} & [0]_{5\times5} & \frac{1}{\theta}[I]_{5\times5} & [0]_{5\times5} \\ \frac{(1-p)}{\gamma}[I]_{5\times5} & [0]_{5\times5} & \frac{1}{\gamma}[I]_{5\times5} & \frac{1}{\gamma}[I]_{5\times5} \end{bmatrix} \end{array}$$

Multiplying F and V^{-1}, we obtained the following matrix

$$\begin{array}{c} \\ E_a \\ A_a \\ P_a \\ I_a \end{array} \begin{array}{c} \begin{array}{cccc} E_a & A_a & P_a & I_a \end{array} \\ \begin{bmatrix} \beta[K_r]_{5\times5}D & \beta[K_r]_{5\times5}\left(\frac{\alpha}{\gamma_A}\right) & \beta[K_r]_{5\times5}\left(\frac{1}{\theta}+\frac{\kappa}{\gamma}\right) & \beta[K_r]_{5\times5}\left(\frac{\kappa}{\gamma}\right) \\ [0]_{5\times5} & [0]_{5\times5} & [0]_{5\times5} & [0]_{5\times5} \\ [0]_{5\times5} & [0]_{5\times5} & [0]_{5\times5} & [0]_{5\times5} \\ [0]_{5\times5} & [0]_{5\times5} & [0]_{5\times5} & [0]_{5\times5} \end{bmatrix} \end{array}$$

where

$$D = \left(\frac{\alpha p}{\gamma_A} + \frac{\zeta(1-p)}{\theta} + \frac{\kappa(1-p)}{\gamma}\right)$$

Then the spectral radius of FV^{-1}, defined as the reproduction number, is given by $R_0 = \beta[K_r]_{5\times5}D$.

4.4 Derivation of the Control Reproduction Number

We now calculate the effective reproduction, R_e, for the model without re-infection. In this case, we include isolation in the model. Without re-infections, R_e for the age structured model in (4.3) can be derived in a similar manner to R_0. In this case, the infected compartments are E, A, P, I, and Q, leading to matrices of size 25×25.

$$\begin{aligned} S_a' &= -S_a \mathscr{J}_a \\ E_a' &= S_a \mathscr{J}_a - \sigma E_a \\ A_a' &= p\sigma E_a - \gamma_A A_a \\ P_a' &= (1-p)\sigma E_a - \theta P_a \\ I_a' &= (1-q)\theta P_a - \gamma I_a \\ Q_a' &= q\theta P_a - \gamma Q_a \\ R_a' &= \gamma_A A_a + \gamma Q_a + \gamma I_a \end{aligned} \tag{4.3}$$

with

$$\mathscr{J}_a = \beta \sum_{j=1}^{5} M_a^R \left(\frac{\alpha A_j + P_j + \kappa I_j}{N_j} \right) + M_a^I \left(\frac{Q_j}{N_j} \right)$$

Linearizing (4.3) about the DFE, $(S_a(0), 0, 0, ..., 0)$ gives

$$E_a' = \beta S_a(0) \sum_{i=1}^{5} M_{a,i}^R \left(\frac{\alpha A_i + \zeta P_i + \kappa I_i}{N_i} \right) + M_{a,i}^I \left(\frac{Q_i}{N_i} \right) - \sigma E_a$$

$$A_a' = p\sigma E_a - \gamma_A A_a$$

$$P_a' = (1-p)\sigma E_a - \theta P_a$$

$$I_a' = (1-q)\theta P_a - \gamma I_a$$

$$Q_a' = q\theta P_a - \gamma Q_a$$

where R^R and M^I are the regular and isolation contact matrices. Let us define:

$$K_q = \begin{bmatrix} \frac{M_{1,1}^I S_1(0)}{N_1} & \frac{M_{1,2}^I S_1(0)}{N_2} & \frac{M_{1,3}^I S_1(0)}{N_3} & \frac{M_{1,4}^I S_1(0)}{N_4} & \frac{M_{1,5}^I S_1(0)}{N_5} \\ \frac{M_{2,1}^I S_2(0)}{N_1} & \frac{M_{2,2}^I S_2(0)}{N_2} & \frac{M_{2,3}^I S_2(0)}{N_3} & \frac{M_{2,4}^I S_2(0)}{N_4} & \frac{M_{2,5}^I S_2(0)}{N_5} \\ \frac{M_{3,1}^I S_3(0)}{N_1} & \frac{M_{3,2}^I S_3(0)}{N_2} & \frac{M_{3,3}^I S_3(0)}{N_3} & \frac{M_{3,4}^I S_3(0)}{N_4} & \frac{M_{3,5}^I S_3(0)}{N_5} \\ \frac{M_{4,1}^I S_4(0)}{N_1} & \frac{M_{4,2}^I S_4(0)}{N_2} & \frac{M_{4,3}^I S_4(0)}{N_3} & \frac{M_{4,4}^I S_4(0)}{N_4} & \frac{M_{4,5}^I S_4(0)}{N_5} \\ \frac{M_{5,1}^I S_5(0)}{N_1} & \frac{M_{5,2}^I S_5(0)}{N_2} & \frac{M_{5,3}^I S_5(0)}{N_3} & \frac{M_{5,4}^I S_5(0)}{N_4} & \frac{M_{5,5}^I S_5(0)}{N_5} \end{bmatrix}$$

Then the matrix, $F_{25\times25}$ becomes

$$F_{25\times25} = \begin{array}{c} \\ E_a \\ A_a \\ P_a \\ I_a \\ Q_a \end{array} \begin{array}{c} \begin{array}{ccccc} E_a & A_a & P_a & I_a & Q_a \end{array} \\ \begin{bmatrix} [0]_{5\times5} & \beta\alpha\,[K_r]_{5\times5} & \beta\,[K_r]_{5\times5} & \beta\kappa\,[K_r]_{5\times5} & \beta\kappa\,[K_q]_{5\times5} \\ [0]_{5\times5} & [0]_{5\times5} & [0]_{5\times5} & [0]_{5\times5} & [0]_{5\times5} \\ [0]_{5\times5} & [0]_{5\times5} & [0]_{5\times5} & [0]_{5\times5} & [0_{5\times5} \\ [0]_{5\times5} & [0]_{5\times5} & [0]_{5\times5} & [0]_{5\times5} & [0]_{5\times5} \\ [0]_{5\times5} & [0]_{5\times5} & [0]_{5\times5} & [0]_{5\times5} & [0]_{5\times5} \end{bmatrix} \end{array}$$

and we have

$$V_{25\times25} = \begin{array}{c} \\ E_a \\ A_a \\ P_a \\ I_a \\ Q_a \end{array} \begin{array}{c} \begin{array}{ccccc} E_a & A_a & P_a & I_a & Q_a \end{array} \\ \begin{bmatrix} \sigma[I]_{5\times5} & [0]_{5\times5} & [0]_{5\times5} & [0]_{5\times5} & [0]_{5\times5} \\ -p\sigma[I]_{5\times5} & \gamma_A[I]_{5\times5} & [0]_{5\times5} & [0]_{5\times5} & [0]_{5\times5} \\ -(1-p)\sigma[I]_{5\times5} & [0]_{5\times5} & \theta[I]_{5\times5} & [0]_{5\times5} & [0]_{5\times5} \\ [0]_{5\times5} & [0]_{5\times5} & -(1-q)\theta[I]_{5\times5} & \gamma[I]_{5\times5} & [0]_{5\times5} \\ [0]_{5\times5} & [0]_{5\times5} & -q\theta[I]_{5\times5} & \gamma[I]_{5\times5} & \end{bmatrix} \end{array}$$

It then follows that

$$V_{25\times25}^{-1} = \begin{array}{c} \\ E_a \\ A_a \\ P_a \\ I_a \\ Q_a \end{array} \begin{array}{c} \begin{array}{ccccc} E_a & A_a & P_a & I_a & Q_a \end{array} \\ \begin{bmatrix} \frac{1}{\sigma}[I]_{5\times5} & [0]_{5\times5} & [0]_{5\times5} & [0]_{5\times5} & [0]_{5\times5} \\ \frac{p}{\gamma_A}[I]_{5\times5} & \frac{1}{\gamma_A}[I]_{5\times5} & [0]_{5\times5} & [0]_{5\times5} & [0]_{5\times5} \\ \frac{(1-p)}{\theta}\sigma[I]_{5\times5} & [0]_{5\times5} & \frac{1}{\theta}[I]_{5\times5} & [0]_{5\times5} & [0]_{5\times5} \\ \frac{(1-p)(1-q)}{\gamma}[I]_{5\times5} & [0]_{5\times5} & \frac{(1-q)}{\gamma}[I]_{5\times5} & \frac{1}{\gamma}[I]_{5\times5} & [0]_{5\times5} \\ \frac{(1-p)q}{\gamma}[I]_{5\times5} & [0]_{5\times5} & \frac{q}{\gamma}[I]_{5\times5} & [0]_{5\times5} & \frac{1}{\gamma}[I]_{5\times5} \end{bmatrix} \end{array}$$

Calculating FV^{-1}, the control reproduction number R_e in the presence of only isolation is expressed by

$$R_e = \beta\left(\frac{\alpha p}{\gamma_A} + \frac{\zeta(1-p)}{\theta} + \frac{\kappa(1-p)(1-q)}{\gamma}\right)[K_r]_{5\times5} + \beta\left(\frac{\kappa q(1-p)}{\gamma}\right)[K_q]_{5\times5}$$

in which we take the maximum eigenvalues of the matrices K_r and K_q.

A similar approach can be taken to calculate the control reproduction number for the general model (4.1). Using E_a, $E_{r,a}$, A_a, P_a, I_a, and Q_a as infected compartments, and linearizing (4.1) around the DFE $(S_a(0), W_a(0), 0, 0, ..., 0, 0)$, we obtain

$$E_a' = \beta S_a(0)\sum_{i=1}^{5} M_{a,i}^R\left(\frac{\alpha A_i + \zeta P_i + \kappa I_i}{N_i}\right) + M_{a,i}^I\left(\frac{Q_i}{N_i}\right) - \sigma E_a$$

$$E_{r,a}' = \beta W_a(0)\sum_{i=1}^{5} M_{a,i}^R\left(\frac{\alpha A_i + \zeta P_i + \kappa I_i}{N_i}\right) + M_{a,i}^I\left(\frac{Q_i}{N_i}\right) - \sigma E_{r,a}$$

$$A_a' = p\sigma E_a + p_r\sigma E_{r,a} - \gamma_A A_a$$

$$P_a' = (1-p)\sigma E_a + (1-p_r)E_{r,a} - \theta P_a$$

$$I_a' = (1-q)\theta P_a - \gamma I_a$$

$$Q_a' = q\theta P_a - \gamma Q_a$$

Let us define:

$$K_{rs} = \begin{bmatrix} \frac{M^R_{1,1}S_1(0)}{N_1} & \frac{M^R_{1,2}S_1(0)}{N_2} & \frac{M^R_{1,3}S_1(0)}{N_3} & \frac{M^R_{1,4}S_1(0)}{N_4} & \frac{M^R_{1,5}S_1(0)}{N_5} \\ \frac{M^R_{2,1}S_2(0)}{N_1} & \frac{M^R_{2,2}S_2(0)}{N_2} & \frac{M^R_{2,3}S_2(0)}{N_3} & \frac{M^R_{2,4}S_2(0)}{N_4} & \frac{M^R_{2,5}S_2(0)}{N_5} \\ \frac{M^R_{3,1}S_3(0)}{N_1} & \frac{M^R_{3,2}S_3(0)}{N_2} & \frac{M^R_{3,3}S_3(0)}{N_3} & \frac{M^R_{3,4}S_3(0)}{N_4} & \frac{M^R_{3,5}S_3(0)}{N_5} \\ \frac{M^R_{4,1}S_4(0)}{N_1} & \frac{M^R_{4,2}S_4(0)}{N_2} & \frac{M^R_{4,3}S_4(0)}{N_3} & \frac{M^R_{4,4}S_4(0)}{N_4} & \frac{M^R_{4,5}S_4(0)}{N_5} \\ \frac{M^R_{5,1}S_5(0)}{N_1} & \frac{M^R_{5,2}S_5(0)}{N_2} & \frac{M^R_{5,3}S_5(0)}{N_3} & \frac{M^R_{5,4}S_5(0)}{N_4} & \frac{M^R_{5,5}S_5(0)}{N_5} \end{bmatrix}$$

$$K_{qs} = \begin{bmatrix} \frac{M^I_{1,1}S_1(0)}{N_1} & \frac{M^I_{1,2}S_1(0)}{N_2} & \frac{M^I_{1,3}S_1(0)}{N_3} & \frac{M^I_{1,4}S_1(0)}{N_4} & \frac{M^I_{1,5}S_1(0)}{N_5} \\ \frac{M^I_{2,1}S_2(0)}{N_1} & \frac{M^I_{2,2}S_2(0)}{N_2} & \frac{M^I_{2,3}S_2(0)}{N_3} & \frac{M^I_{2,4}S_2(0)}{N_4} & \frac{M^I_{2,5}S_2(0)}{N_5} \\ \frac{M^I_{3,1}S_3(0)}{N_1} & \frac{M^I_{3,2}S_3(0)}{N_2} & \frac{M^I_{3,3}S_3(0)}{N_3} & \frac{M^I_{3,4}S_3(0)}{N_4} & \frac{M^I_{3,5}S_3(0)}{N_5} \\ \frac{M^I_{4,1}S_4(0)}{N_1} & \frac{M^I_{4,2}S_4(0)}{N_2} & \frac{M^I_{4,3}S_4(0)}{N_3} & \frac{M^I_{4,4}S_4(0)}{N_4} & \frac{M^I_{4,5}S_4(0)}{N_5} \\ \frac{M^I_{5,1}S_5(0)}{N_1} & \frac{M^I_{5,2}S_5(0)}{N_2} & \frac{M^I_{5,3}S_5(0)}{N_3} & \frac{M^I_{5,4}S_5(0)}{N_4} & \frac{M^I_{5,5}S_5(0)}{N_5} \end{bmatrix}$$

$$K_{rw} = \begin{bmatrix} \frac{M^R_{1,1}W_1(0)}{N_1} & \frac{M^R_{1,2}W_1(0)}{N_2} & \frac{M^R_{1,3}W_1(0)}{N_3} & \frac{M^R_{1,4}W_1(0)}{N_4} & \frac{M^R_{1,5}W_1(0)}{N_5} \\ \frac{M^R_{2,1}W_2(0)}{N_1} & \frac{M^R_{2,2}W_2(0)}{N_2} & \frac{M^R_{2,3}W_2(0)}{N_3} & \frac{M^R_{2,4}W_2(0)}{N_4} & \frac{M^R_{2,5}W_2(0)}{N_5} \\ \frac{M^R_{3,1}W_3(0)}{N_1} & \frac{M^R_{3,2}W_3(0)}{N_2} & \frac{M^R_{3,3}W_3(0)}{N_3} & \frac{M^R_{3,4}W_3(0)}{N_4} & \frac{M^R_{3,5}W_3(0)}{N_5} \\ \frac{M^R_{4,1}W_4(0)}{N_1} & \frac{M^R_{4,2}W_4(0)}{N_2} & \frac{M^R_{4,3}W_4(0)}{N_3} & \frac{M^R_{4,4}W_4(0)}{N_4} & \frac{M^R_{4,5}W_4(0)}{N_5} \\ \frac{M^R_{5,1}W_5(0)}{N_1} & \frac{M^R_{5,2}W_5(0)}{N_2} & \frac{M^R_{5,3}W_5(0)}{N_3} & \frac{M^R_{5,4}W_5(0)}{N_4} & \frac{M^R_{5,5}W_5(0)}{N_5} \end{bmatrix}$$

$$K_{qw} = \begin{bmatrix} \frac{M^I_{1,1}W_1(0)}{N_1} & \frac{M^I_{1,2}W_1(0)}{N_2} & \frac{M^I_{1,3}W_1(0)}{N_3} & \frac{M^I_{1,4}W_1(0)}{N_4} & \frac{M^I_{1,5}W_1(0)}{N_5} \\ \frac{M^I_{2,1}W_2(0)}{N_1} & \frac{M^I_{2,2}W_2(0)}{N_2} & \frac{M^I_{2,3}W_2(0)}{N_3} & \frac{M^I_{2,4}W_2(0)}{N_4} & \frac{M^I_{2,5}W_2(0)}{N_5} \\ \frac{M^I_{3,1}W_3(0)}{N_1} & \frac{M^I_{3,2}W_3(0)}{N_2} & \frac{M^I_{3,3}W_3(0)}{N_3} & \frac{M^I_{3,4}W_3(0)}{N_4} & \frac{M^I_{3,5}W_3(0)}{N_5} \\ \frac{M^I_{4,1}W_4(0)}{N_1} & \frac{M^I_{4,2}W_4(0)}{N_2} & \frac{M^I_{4,3}W_4(0)}{N_3} & \frac{M^I_{4,4}W_4(0)}{N_4} & \frac{M^I_{4,5}W_4(0)}{N_5} \\ \frac{M^I_{5,1}W_5(0)}{N_1} & \frac{M^I_{5,2}W_5(0)}{N_2} & \frac{M^I_{5,3}W_5(0)}{N_3} & \frac{M^I_{5,4}W_5(0)}{N_4} & \frac{M^I_{5,5}W_5(0)}{N_5} \end{bmatrix}$$

Then $F_{30\times30}$ is given by

$$\begin{array}{c} \\ E_a \\ E_{r,a} \\ A_a \\ 0P_a \\ I_a \\ Q_a \end{array} \begin{array}{c} \begin{array}{cccccc} E_a & E_{r,a} & A_a & P_a & I_a & Q_a \end{array} \\ \begin{bmatrix} [0]_{5\times5} & [0]_{5\times5} & \beta\alpha\,[K_r s]_{5\times5} & \beta\,[K_r s]_{5\times5} & \beta\kappa[K_r s]_{5\times5} & \beta\kappa\,[K_q s]_{5\times5} \\ [0]_{5\times5} & [0]_{5\times5} & \beta\alpha\,[K_r w]_{5\times5} & \beta\,[K_r w]_{5\times5} & \beta\kappa\,[K_r w]_{5\times5} & \beta\kappa\,[K_q w]_{5\times5} \\ [0]_{5\times5} & [0]_{5\times5} & [0]_{5\times5} & [0]_{5\times5} & [0]_{5\times5} & [0]_{5\times5} \\ [0]_{5\times5} & [0]_{5\times5} & [0]_{5\times5} & [0]_{5\times5} & [0_{5\times5} & [0]_{5\times5} \\ [0]_{5\times5} & [0]_{5\times5} & [0]_{5\times5} & [0]_{5\times5} & [0]_{5\times5} & [0]_{5\times5} \\ [0]_{5\times5} & [0]_{5\times5} & [0]_{5\times5} & [0]_{5\times5} & [0]_{5\times5} & [0]_{5\times5} \end{bmatrix} \end{array}$$

and $V_{30\times30}$ is

$$\begin{array}{c} \\ E_a \\ E_{r,a} \\ A_a \\ P_a \\ I_a \\ Q_a \end{array} \begin{array}{c} \begin{array}{cccccc} E_a & E_{r,a} & A_a & P_a & I_a & Q_a \end{array} \\ \begin{bmatrix} \sigma[I]_{5\times5} & [0]_{5\times5} & [0]_{5\times5} & [0]_{5\times5} & [0]_{5\times5} & [0]_{5\times5} \\ [0]_{5\times5} & \sigma[I]_{5\times5} & [0]_{5\times5} & [0]_{5\times5} & [0]_{5\times5} & [0]_{5\times5} \\ -p\sigma[I]_{5\times5} & -p_r\sigma[I]_{5\times5} & \gamma_A[I]_{5\times5} & [0]_{5\times5} & [0]_{5\times5} & [0]_{5\times5} \\ -(1-p)\sigma[I]_{5\times5} & -(1-p_r)\sigma[I]_{5\times5} & [0]_{5\times5} & \theta[I]_{5\times5} & [0]_{5\times5} & [0]_{5\times5} \\ [0]_{5\times5} & [0]_{5\times5} & [0]_{5\times5} & -(1-q)\theta[I]_{5\times5} & \gamma[I]_{5\times5} & [0]_{5\times5} \\ [0]_{5\times5} & [0]_{5\times5} & [0]_{5\times5} & -q\theta[I]_{5\times5} & [0]_{5\times5} & \gamma[I]_{5\times5} \end{bmatrix} \end{array}$$

Calculating FV^{-1} gives

$$FV^{-1} = \begin{bmatrix} A & B \\ C & D \end{bmatrix}$$

where

$$A = \beta\left(\frac{\alpha p}{\gamma_A} + \frac{\zeta(1-p)}{\theta} + \frac{k(1-p)(1-q)}{\gamma}\right)[K_{rs}]_{5\times5} + \beta\left(\frac{\kappa q(1-p)}{\gamma}\right)[K_{qs}]_{5\times5},$$
$$B = \beta\left(\frac{\alpha p}{\gamma_A} + \frac{\zeta(1-p)}{\theta} + \frac{k(1-p)(1-q)}{\gamma}\right)[K_{rs}]_{5\times5} + \beta\left(\frac{\kappa q(1-p)}{\gamma}\right)[K_{qs}]_{5\times5},$$
$$C = \beta\left(\frac{\alpha p}{\gamma_A} + \frac{\zeta(1-p)}{\theta} + \frac{k(1-p)(1-q)}{\gamma}\right)[K_{rw}]_{5\times5} + \beta\left(\frac{\kappa q(1-p)}{\gamma}\right)[K_{qw}]_{5\times5},$$
$$D = \beta\left(\frac{\alpha p_r}{\gamma_A} + \frac{\zeta(1-p_r)}{\theta} + \frac{k(1-p_r)(1-q)}{\gamma}\right)[K_{rw}]_{5\times5} + \beta\left(\frac{\kappa q(1-p_r)}{\gamma}\right)[K_{qw}]_{5\times5}$$

Thus, the control reproduction number is given by the spectral radius of this matrix.

4.5 Deterministic Implementation

For the deterministic model (4.3), 200 simulations were run where independent samples were drawn from parameter distributions associated with infectious periods in different stages of the disease, while fixing the parameters β, p, q, α, ζ, and κ. The fixed parameters were obtained from the literature. The other parameters in the model, σ, γ_A, γ, and θ were sampled 200 times from their distributions derived from the published studies. Tables 4.3 and 4.4 includes the model parameters. The baseline model without isolation was calibrated to an attack rate of 55% [70] to obtain the transmissibility, β, for both Influenza (A/H1N1 strain) and SARS-CoV-2 original strain. For the Alpha variant, β was determined using the estimated relative transmissibility, which is ~ 1.5 times more transmissible than SARS-CoV-2 original strain [25, 26]. Further, the Delta variant was estimated to be 1.3 times more transmissible than the Alpha variant [28, 29]. Finally, the Omicron variant was estimated to be 1.35 times as transmissible as the Delta variant [30].

The forward Euler method was used with a step size of 0.05 to simulate the model in Matlab©. The incidence, cumulative incidence, and attack rate (i.e., the proportion of pop-

Table 4.3: Model parameters that are fixed in simulations.

	Influenza	SARS-CoV-2 Varinats				
Parameter	**H1N1**	**Original**	**Alpha**	**Delta**	**Omicron**	**Reference**
β	0.029	0.032	0.048	0.0624	0.08424	—
p	0.50	0.351	0.351	0.351	0.351	[43, 49, 50]
q	0.50	0.50	0.50	0.50	0.50	—
α	0.50	0.26	0.26	0.26	0.26	[11]
ζ	0.80	1.00	1.00	1.00	1.00	[11]
κ	1.00	0.89	0.89	0.89	0.89	[11]

ulation infected over the simulation time interval) were plotted for temporal observations in the 20 different scenarios considered. Further, the relative reduction (RR) in the attack rate for each intervention was plotted to determine which intervention resulted in the largest impact on disease control. Note that interventions are implemented at the start of simulation and maintained through the entire simulation period of 365 days. Uncertainty ranges were computed by bootstrapping the simulation outcomes for the overall and age-specific attack rates using the mean function, with 500 replications of the same sample size (200) that were randomly generated. The bias corrected and accelerated percentile method [71] involves a z_0 factor computed using the proportion of bootstrap values that are less than the original sample value. To produce reasonable results when the sample is lumpy, z_0 is computed by including half of the bootstrap values that are the same as the original sample value. This method corrects for bias and skewness in the distribution of bootstrap estimates when scaled from the per capita to the entire population. The baseline scenario was used as a reference for the relative reduction in the attack rate. The general formula describing the vector calculation of the RR is expressed by

$$\mathrm{RR} = \frac{\text{Total Incidence}_{\text{(baseline)}} - \text{Total Incidence}_{\text{(intervention)}}}{\text{Total Incidence}_{\text{(baseline)}}}$$

4.5.1 Sensitivity Analysis

To determine which parameters have the greatest influence on the relative reduction in attack rate, a sensitivity analysis was performed using the sampled simulations to determine the Partial Rank Correlation Coefficient (PRCC). These were computed and plotted for each type of infection and intervention. R version 3.5.3 was used to conduct the sensitivity analysis. PRCCs were computed using the epiR package (v2.0.56; Stevens et al. 2023) and the sensitivity package (v1.6-1; Pujol, Iooss, & Janon 2013) [72, 73].

Table 4.4: Model parameters sampled from their respective distributions truncated within estimated ranges.

Infection Parameters [Truncation]					
Influenza	σ	γ_A	γ	θ	Reference
H1N1	$\mathrm{U}(1,2)$	$\log\mathrm{N}(1,0.4356)$	$\log\mathrm{N}(1,0.4356)$	$\log\mathrm{N}(-0.775,0.16)$	[74]
	$[1,2]$	$[3,7]$	$[3,7]$	$[0.2,0.8]$	
SARS-CoV-2					
Original	$\mathrm{N}(2.2,0.4)$	$\mathrm{G}(5,1)$	$\mathrm{G}(2.768,1.1563)$	$\mathrm{G}(1.058,2.174)$	[63]
	$[1,3]$	$[3,7]$	$[2,5]$	$[0.8,3.0]$	
Alpha	$\mathrm{N}(2.2,0.4)$	$\mathrm{G}(5,1)$	$\mathrm{G}(2.768,1.1563)$	$\mathrm{G}(1.058,2.174)$	[63]
	$[1,3]$	$[3,7]$	$[2,5]$	$[0.8,3.0]$	
Delta	$\log\mathrm{N}(1.249,0.649)$	$\mathrm{G}(5,1)$	$\mathrm{G}(2.768,1.1563)$	$\mathrm{G}(1.015,1.975)$	[63]
	$[3.5,7]$	$[3,7]$	$[2,5]$	$[0.8,2.2]$	
Omicron	$\log\mathrm{N}(0.99,0.64)$	$\mathrm{G}(5,1)$	$\mathrm{G}(2.768,1.1563)$	$\mathrm{G}(1.015,1.975)$	[63]
	$[3,7]$	$[3,7]$	$[2,5]$	$[0.8,2.2]$	

$\log$N: LogNormal distribution

N: Normal distribution

U: Uniform distribution

G: Gamma distribution

4.6 Stochastic Implementation

To implement the model stochastically, the Markov Chain Monte Carlo (MCMC) algorithm was applied. For the model (4.1), there were twelve possible events for each of the five age groups, resulting in a total of sixty possible events at each step of the random process. The MCMC algorithm uses a random number between 0 and 1 to determine which event will occur.

Considering time t as a continuous variable, we define the following random vector for $t \in [0,\infty)$:

$$\vec{X}(t) = [S_a, E_a, A_a, P_a, I_a, Q_a, R_a, W_a, E_{r,a}](t),$$

and let $\Delta\vec{X}(t) = \vec{X}(t+\Delta t) - \vec{X}(t)$. Thus, the transition probability associated with the movement of individuals between the model compartments during the time interval Δt is defined as

$$P[\Delta\vec{X}(t) = \big(\Theta(S_a), \Theta(E_a), \Theta(A_a), \Theta(P_a), \Theta(I_a), \Theta(Q_a), \Theta(R_a), \Theta(W_a), \Theta(E_{r,a})\big)\big|\vec{X}(t)],$$

where

$$\Theta(\cdot) = \begin{cases} -1 & \text{decrease in class } (\cdot) \\ 0 & \text{no change in class } (\cdot) \\ +1 & \text{increase in class } (\cdot) \end{cases}$$

The function $\Theta(\cdot)$ describes the change in the status of an individual in the population by moving from one class to another during the time interval Δt. It is assumed that Δt is sufficiently small to allow for the occurrence of at most one change in every state of the model. Thus, the corresponding continuous time Markov chain model is fully described through the possible transition rates as described below.

1. A susceptible individual becomes infected:

$$[S,E,A,P,I,Q,R,W,E_r] \to [S-1,E+1,A,P,I,Q,R,W,E_r]$$

2. An infected individual moves to the pre-symptomatic stage:

$$[S,E,A,P,I,Q,R,W,E_r] \to [S,E-1,A,P+1,I,Q,R,W,E_r]$$

3. An infected individual moves to the asymptomatic stage:

$$[S,E,A,P,I,Q,R,W,E_r] \to [S,E-1,A+1,P,I,Q,R,W,E_r]$$

4. An individual in the pre-symptomatic stage moves to the symptomatic stage:

$$[S,E,A,P,I,Q,R,W,E_r] \to [S,E,A,P-1,I+1,Q,R,W,E_r]$$

5. A pre-symptomatic, infectious individual self-isolates:

$$[S,E,A,P,I,Q,R,W,E_r] \to [S,E,A,P-1,I,Q+1,R,W,E_r]$$

6. An asymptomatic individual recovers:

$$[S,E,A,P,I,Q,R,W,E_r] \to [S,E,A-1,P,I,Q,R+1,W,E_r]$$

7. A symptomatic individual recovers:

$$[S,E,A,P,I,Q,R,W,E_r] \to [S,E,A,P,I-1,Q,R+1,W,E_r]$$

8. An isolated individual recovers:

$$[S,E,A,P,I,Q,R,W,E_r] \rightarrow [S,E,A,P,I,Q-1,R+1,W,E_r]$$

9. Immunity of a recovered individual wanes:

$$[S,E,A,P,I,Q,R,W,E_r] \rightarrow [S,E,A,P,I,Q,R-1,W+1,E_r]$$

10. An individual with loss of immunity becomes reinfected:

$$[S,E,A,P,I,Q,R,W,E_r] \rightarrow [S,E,A,P,I,Q,R,W-1,E_r+1]$$

11. A reinfected individual moves to the pre-symptomatic stage:

$$[S,E,A,P,I,Q,R,W,E_r] \rightarrow [S,E,A,P+1,I,Q,R,W,E_r-1]$$

12. A reinfected individual moves to the asymptomatic stage:

$$[S,E,A,P,I,Q,R,W,E_r] \rightarrow [S,E,A+1,P,I,Q,R,W,E_r-1]$$

These twelve events can occur for any age group, giving a total of sixty probabilistic events for all 5 age groups.

4.6.1 Stochastic Parameterization

The fixed parameter values in Table 4.3 were used for the stochastic simulations. However, for other parameters varied in the deterministic model, we used the mean values provided in Table 4.5. Similar to the deterministic model, the baseline stochastic model was calibrated to an attack rate of 55% [70] on a population size of $N = 1,000$ to obtain the transmissibility, β, for Influenza (A/H1N1 strain) and SARS-CoV-2 original strain. The

Table 4.5: Mean of model parameters from their respective distributions shown in Table 4.4 and the calibrated transmissibilities.

Mean Values of Parameters					
Influenza	β	σ	γ_A	γ	θ
H1N1	0.0435	1.5	3.0	3.0	0.46
SARS-CoV-2					
Original	0.033	2.2	5.0	3.2	2.3
Alpha	0.0495	2.2	5.0	3.2	2.3
Delta	0.06435	4.3	5.0	3.2	2.0
Omicron	0.08687	3.3	5.0	3.2	2.0

assumptions on transmissibilities of the Alpha, Delta, and Omicron variants relative to the original Wuhan-I strain were applied [25, 26, 28–30]. These values are included in Table 4.5.

Chapter 5

Results

In this chapter, we present the results from the deterministic simulations using the sampling method provided in Chapter 4 for scenarios of baseline without any interventions, baseline with only isolation (S1), school closure (S2), and lockdown (S3). For each disease, the incidence and cumulative incidence are presented for the overall population, as well as the attack rates by age group. We also present the results of sensitivity analyses using the PRCC for the deterministic model using sampled parameters. Finally, $10,000$ MCMC simulations for each of the scenarios are performed to illustrate the results of the stochastic model for influenza H1N1, SARS-CoV-2 original strain, SARS-CoV-2 Alpha variant, SARS-CoV-2 Delta variant, and SARS-CoV-2 Omicron variant.

5.1 Deterministic Simulations

5.1.1 Influenza: H1N1

Assuming an attack rate of 55% in a totally susceptible population, the baseline transmission rate $\beta = 0.029$ was derived in the calibration of the baseline model. Using fixed parameter values in Table 4.3, and sampled infection parameters, Figure 5.1 illustrates the simulations for incidence and cumulative incidence derived for each scenario. Clearly, as the intensity of interventions, affecting contact patterns in the population, increases,

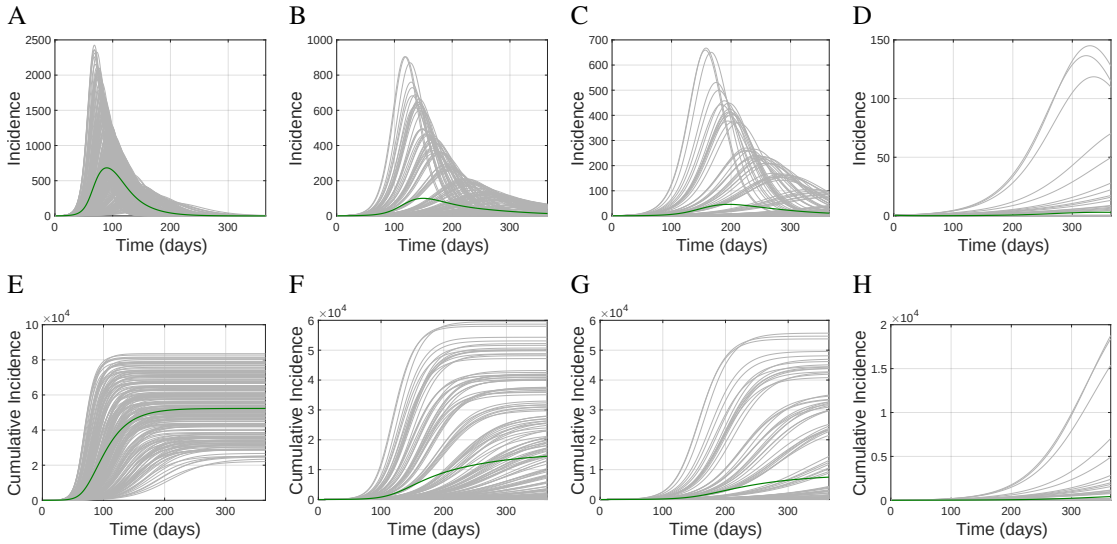

Figure 5.1: Simulated incidence of infection in the population for influenza H1N1 for scenarios of the baseline without any interventions (A); isolation only (B); school closure (C); and lockdown (D). The corresponding cumulative incidence over a period of 365 days for each intervention scenarios are illustrated in panels E–H.

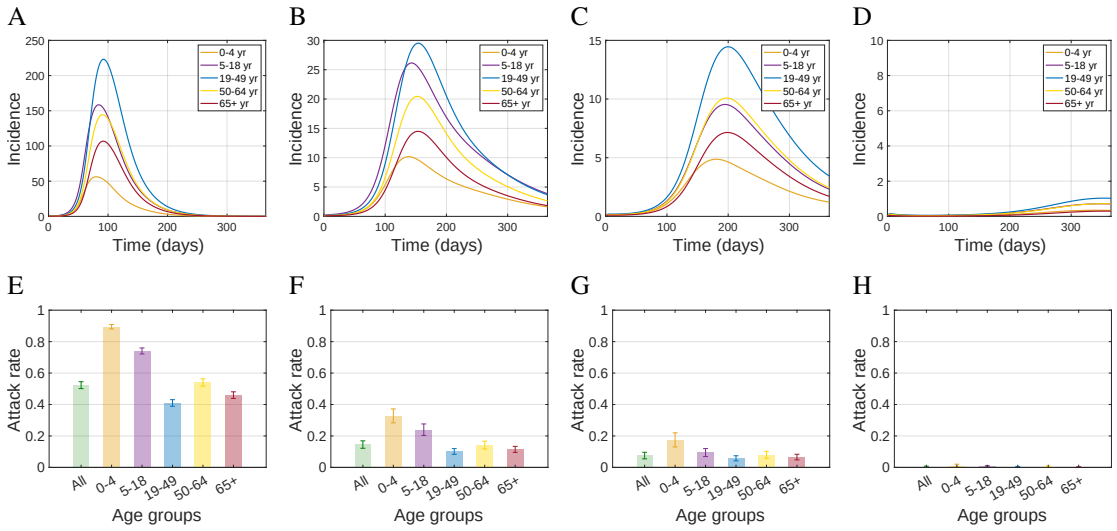

Figure 5.2: Age-specific incidence of infection for influenza H1N1 for scenarios of the baseline without any interventions (A); isolation only (B); school closure (C); and lockdown (D). The corresponding overall and age-specific attack rates over a period of 365 days for each intervention scenarios are illustrated in panels E–H.

the average daily incidence reduces, flattening the curve of infection with further delay in the peak time of the outbreak. This also results in a lower cumulative incidence, and thus reduces the overall attack rate.

We observed a similar trend in the daily incidence of infection among different age groups (Figure 5.2). Not surprisingly, the age group 19–49 has the greatest incidence (due to their larger number of daily contacts) and 0–4 has the smallest number of incident

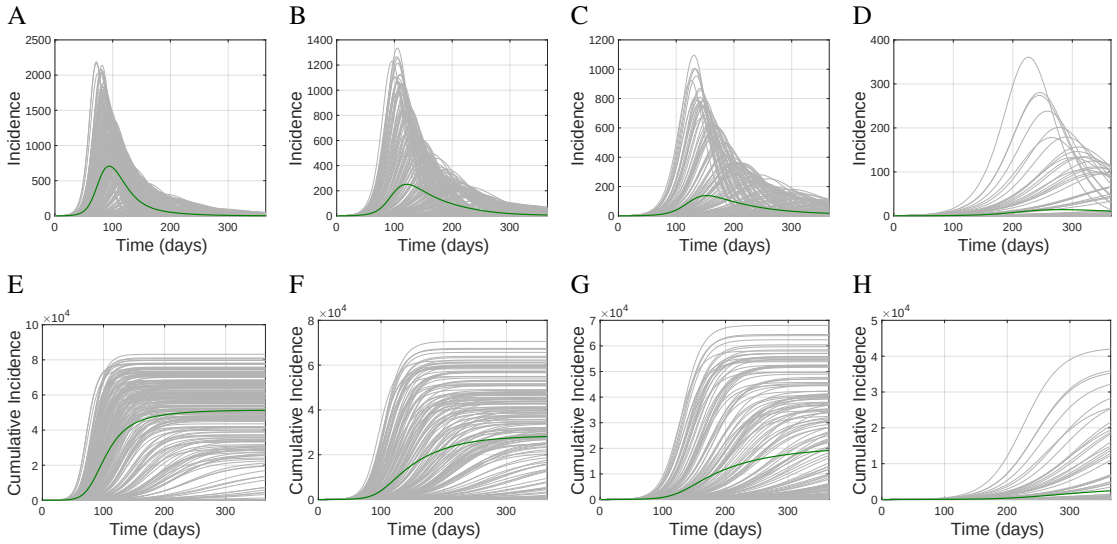

Figure 5.3: Simulated incidence of infection in the population for SARS-CoV-2 original strain for scenarios of the baseline without any interventions (A); isolation only (B); school closure (C); and lockdown (D). The corresponding cumulative incidence over a period of 365 days for each intervention scenarios are illustrated in panels E–H.

infections. The barplots in Figure 5.2 illustrate the attack rate in different age groups, and quantify the effect of interventions on the reduction of the infection in the overall population and among age groups.

5.1.2 SARS-CoV-2: Original Wuhan-I strain

Assuming an attack rate of 55% For the original strain of SARS-CoV-2 in a totally susceptible population, the baseline transmission rate $\beta = 0.032$ was derived in the calibration of the baseline model. Simulations show that there is a similar trend to what was exhibited for influenza for both incidence and attack rates; however, the reduction in the daily and cumulative incidences is lower than that observed for influenza (Figure 5.3). Even with the same attack rate as influenza in the absence of interventions, SARS-CoV-2 results in a higher overall incidence and attack rates among different age groups with interventions (Figure 5.4), indicating that the characteristics of the disease influence intervention outcomes.

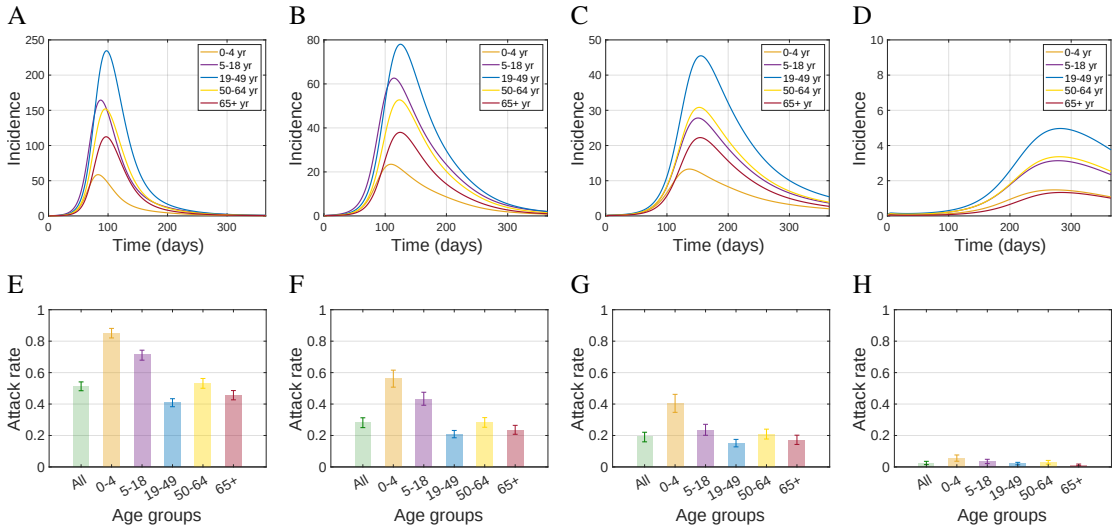

Figure 5.4: Age-specific incidence of infection for SARS-CoV-2 original strain for scenarios of the baseline without any interventions (A); isolation only (B); school closure (C); and lockdown (D). The corresponding overall and age-specific attack rates over a period of 365 days for each intervention scenarios are illustrated in panels E–H.

5.1.3 SARS-CoV-2: Alpha Variant

For the Alpha variant, the baseline transmission rate was increased by 50% to $\beta = 0.048$. Figure 5.5 shows that the effect of interventions is markedly reduced compared to influenza or SARS-CoV-2 original strain. For example, even in the most restrictive measure of lockdown, the overall attack rate is approximately 40%, while it remained below 5% for both influenza SARS-CoV-2 original strain (Figures 5.2 and 5.4). This is notwithstanding the fact that successively more restrictive measures reduces the incidence among different age groups and delays the peak of incidence during the outbreak. However, this delay is significantly shorter compared to the scenarios of influenza and SARS-CoV-2 original strain. For example, the peak of incidence is delayed by about 8 weeks in lockdown compared to baseline (Figure 5.5), while this delay can exceed 200 days for influenza and 150 days for SARS-CoV-2 original strain (Figures 5.1, 5.3). The peak of daily incidence occurs about 110 days into the simulations, with approximately 500 cases for the Alpha variant with lockdown measure (Figure 5.5), whereas there were less than 10 cases at the peak of incidence for both influenza and SARS-CoV-2 original strain with the same intervention (Figure 5.1, 5.3).

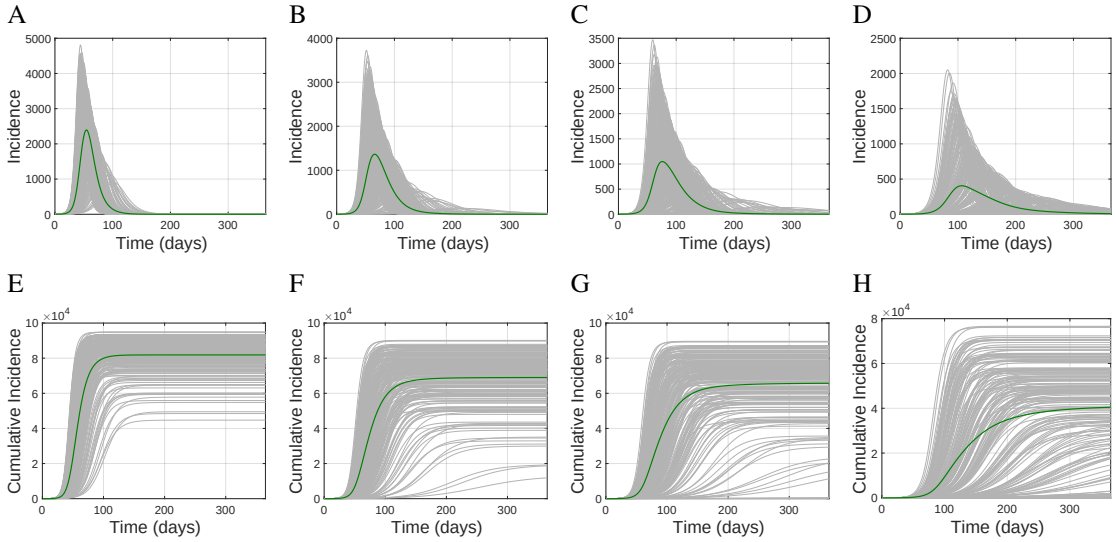

Figure 5.5: Simulated incidence of infection in the population for SARS-CoV-2 Alpha variant for scenarios of the baseline without any interventions (A); isolation only (B); school closure (C); and lockdown (D). The corresponding cumulative incidence over a period of 365 days for each intervention scenarios are illustrated in panels E–H.

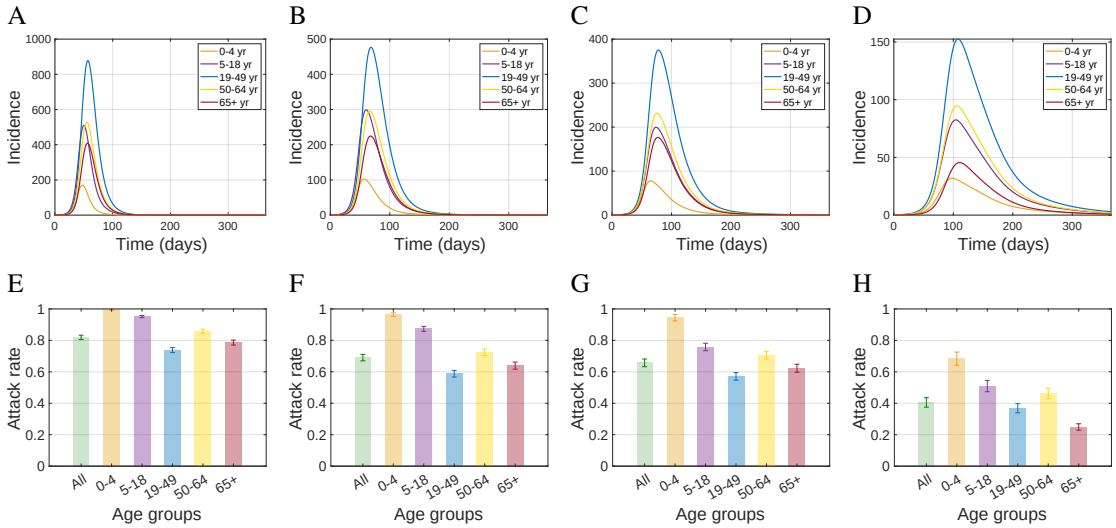

Figure 5.6: Age-specific incidence of infection for SARS-CoV-2 Alpha variant for scenarios of the baseline without any interventions (A); isolation only (B); school closure (C); and lockdown (D). The corresponding overall and age-specific attack rates over a period of 365 days for each intervention scenarios are illustrated in panels E–H.

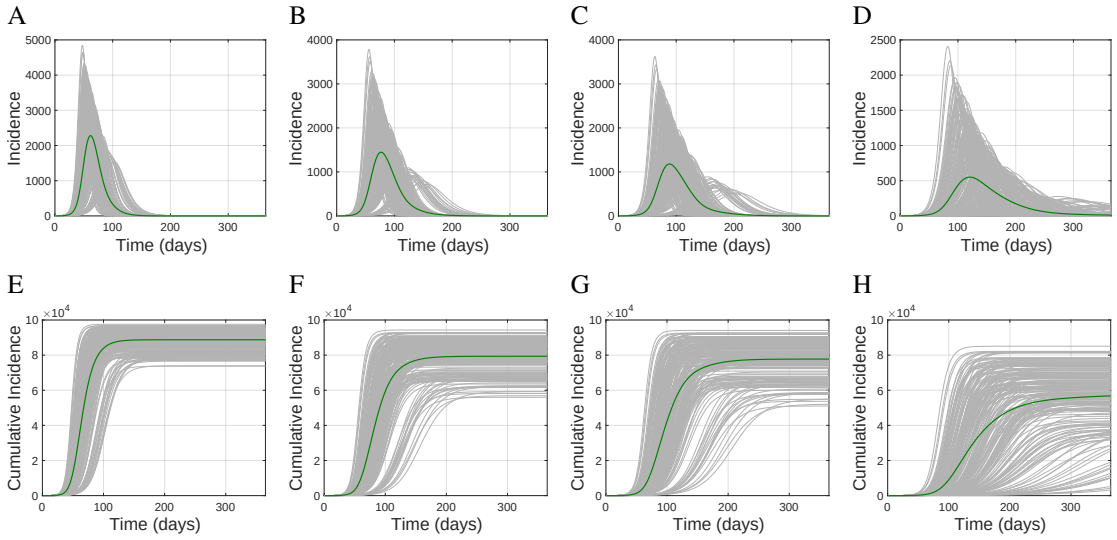

Figure 5.7: Simulated incidence of infection in the population for SARS-CoV-2 Delta variant for scenarios of the baseline without any interventions (A); isolation only (B); school closure (C); and lockdown (D). The corresponding cumulative incidence over a period of 365 days for each intervention scenarios are illustrated in panels E–H.

5.1.4 SARS-CoV-2: Delta Variant

The transmission rate of the Delta variant was assumed to be 30% higher than the Alpha variant, thus giving $\beta = 0.0624$. Compared to the Alpha variant, the effect of intervention was further reduced (Figure 5.7 and 5.8), and the overall attach rate under the lockdown intervention exceeded that of influenza and SARS-CoV-2 original strain in the baseline scenario without any interventions. The timelines for the peak of incidence for different interventions were largely similar to those observed for the Alpha variant; however their magnitudes were increased.

5.1.5 SARS-CoV-2: Omicron Variant

As the most transmissible variant considered in this thesis, the transmission rate for Omicron was set to $\beta = 0.08424$. In addition to a precipitous surge of infections and a significant increase in the peak incidence of disease compared to previous variants (Figure 5.9), the delay in the outbreak peak was minimal with at most 5 weeks delay in lockdown intervention compared to the baseline without any intervention. These simulations indicate that in the absence of other preventive measures such as vaccination, non-pharmaceutical

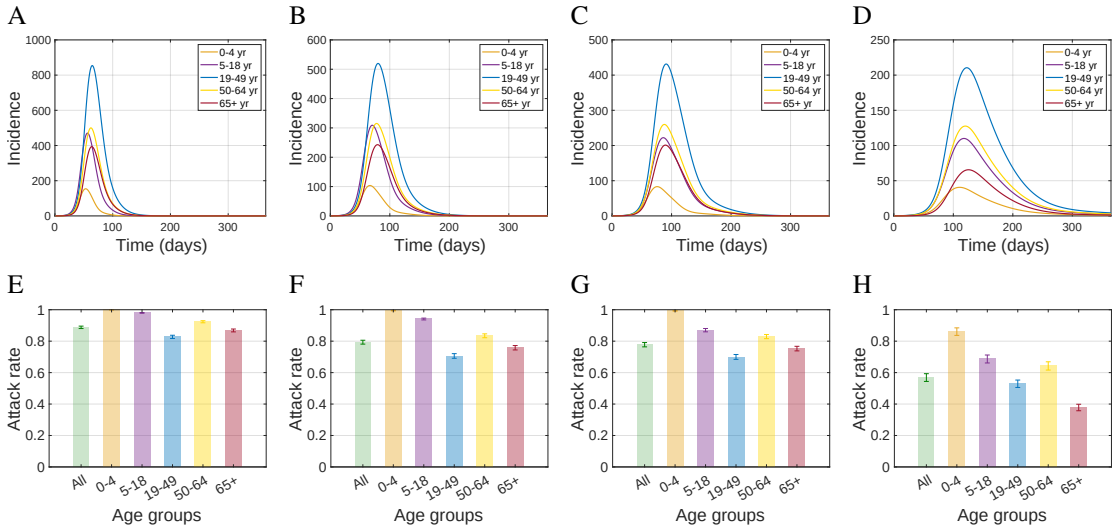

Figure 5.8: Age-specific incidence of infection for SARS-CoV-2 Delta variant for scenarios of the baseline without any interventions (A); isolation only (B); school closure (C); and lockdown (D). The corresponding overall and age-specific attack rates over a period of 365 days for each intervention scenarios are illustrated in panels E–H.

measures would have limited impact on reducing the attack rate of highly transmissible variants (Figure 5.10).

5.1.6 Relative Reduction in Attack Rate

The relative reduction (RR) in attack rate was calculated for interventions of isolation, school closure, and lockdown compared to the baseline without any interventions using

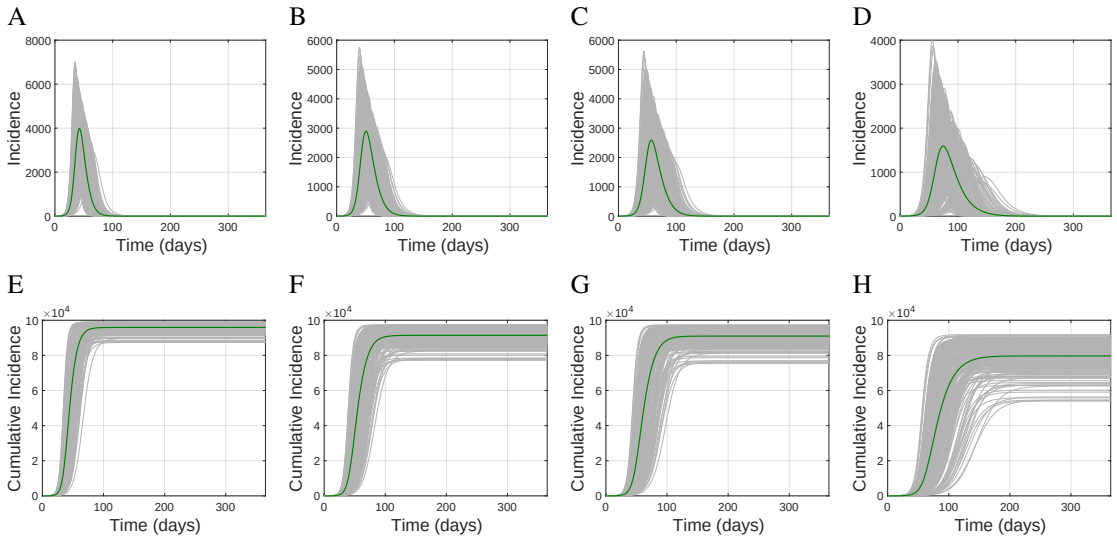

Figure 5.9: Simulated incidence of infection in the population for SARS-CoV-2 Omicron variant for scenarios of the baseline without any interventions (A); isolation only (B); school closure (C); and lockdown (D). The corresponding cumulative incidence over a period of 365 days for each intervention scenarios are illustrated in panels E–H.

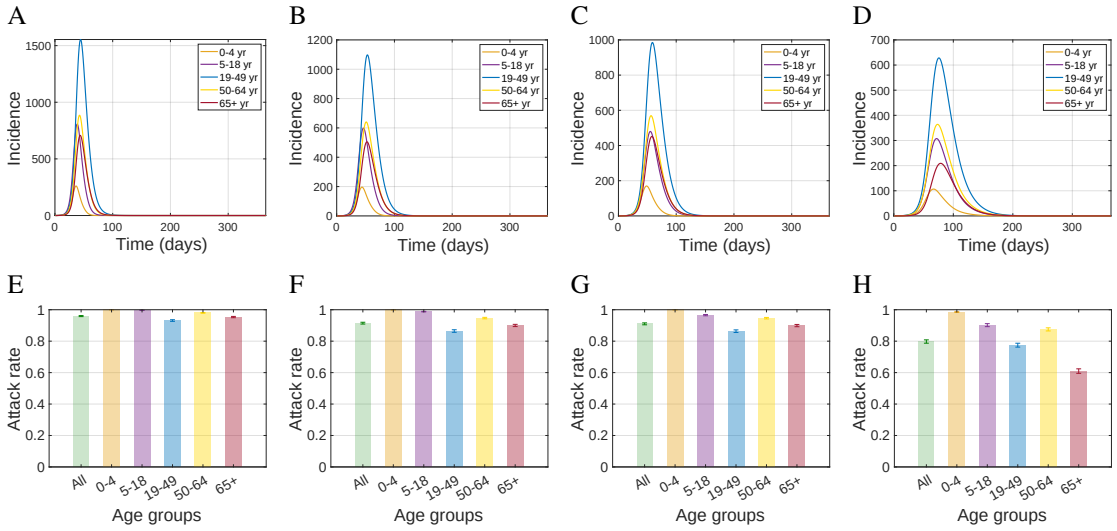

Figure 5.10: Age-specific incidence of infection for SARS-CoV-2 Delta variant for scenarios of the baseline without any interventions (A); isolation only (B); school closure (C); and lockdown (D). The corresponding overall and age-specific attack rates over a period of 365 days for each intervention scenarios are illustrated in panels E–H.

sampled parameters. The RR reaches nearly 100% when lockdown was implemented for influenza. Overall, each intervention had the greatest impact on influenza, with comparatively decreasing effects on variants of SARS-CoV-2 as the transmissibility increased. The lowest impact was observed on the SARS-CoV-2 Omicron variant. Based on the two top plots, it is evident that using school closure as an intervention has the largest impact on children aged 5–18 years old with approximately 2-fold increase compared to isolation only. However, the increase in RR among other age groups is significantly lower, at approximately 20%. The implication is that, overall, isolation on its own is fairly effective for a disease such as SARS-CoV-2 in comparison to influenza.

5.2 Sensitivity Analysis

The PRCC was computed for each of the sampled parameters σ, γ_A, γ, and θ using the RR in attack rate as the response variable. This process was completed for influenza and the variants of SARS-CoV-2 studied here, and for each intervention scenario of isolation, school closure, and lockdown. Barplots and scatter plots are presented in Figures 5.12-5.16 to illustrate the results from this analysis. The parameters with large PRCC values (close

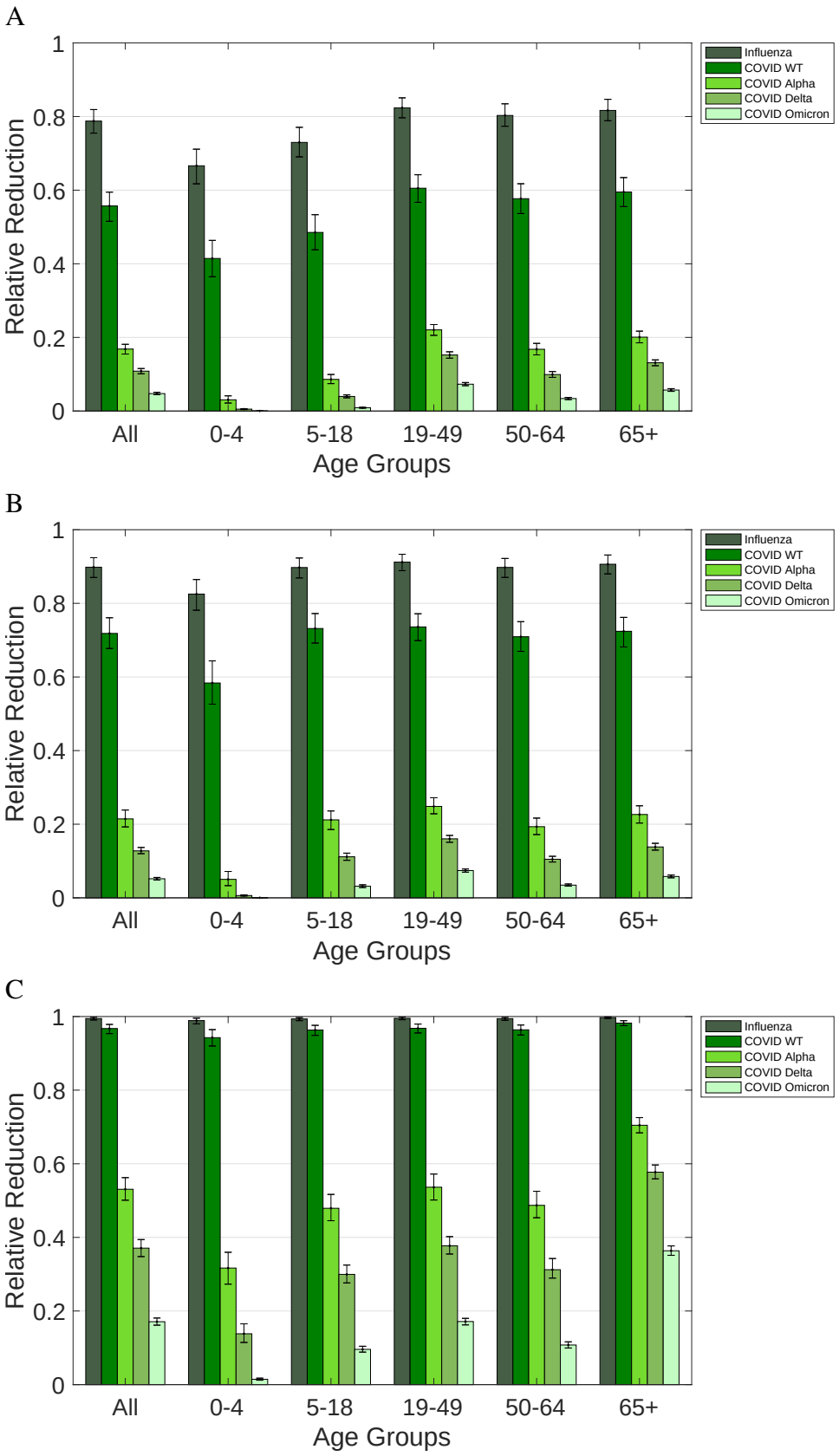

Figure 5.11: Relative reduction of the overall and age-specific attack rates achieved for influenza and variants of SARS-CoV-2 with different interventions of isolation (A); school closure (B), and lockdown (C).

to 1 or -1) and their corresponding p-values smaller than the significance level (0.05) have the greatest influence on the model outcomes [75].

5.2.1 Influenza: H1N1

PRCCs were computed for the four key parameters of σ, γ_A, γ, and θ for each scenario of interventions (Figure 5.12). There is a negative linear correlation between the infectious period, γ, and the RR in attack rate for scenarios isolation, and school closure; however, no strong correlation is apparent between any of the parameters and the intervention of lockdown.

5.2.2 SARS-CoV-2: Wild Type

PRCCs were computed in a similar manner for the original strain of SARS-CoV-2 (Figure 5.13). There is a negative linear correlation between the infectious period, γ, and the RR in attack rate. Furthermore, there is a negative linear relationship between the pre-symptomatic period, θ, and the RR in attack rate for scenarios of isolation and school closure; however, for the scenario of lockdown, the relationships are comparatively weaker.

5.2.3 SARS-CoV-2: Alpha Variant

PRCCs were computed for SARS-CoV-2 Alpha variant (Figure 5.14). In contrast to the original strain of SARS-CoV-2, there is a negative linear correlation between the infectious period, γ, and the RR in attack rate when a lockdown is implemented. There are no significant correlations between other parameters and scenarios of isolation or school closure.

5.2.4 SARS-CoV-2: Delta Variant

PRCCs were computed for SARS-CoV-2 Delta variant (Figure 5.15). There is a moderate, negative linear relationship between the infectious period, γ and the RR in attack rate;

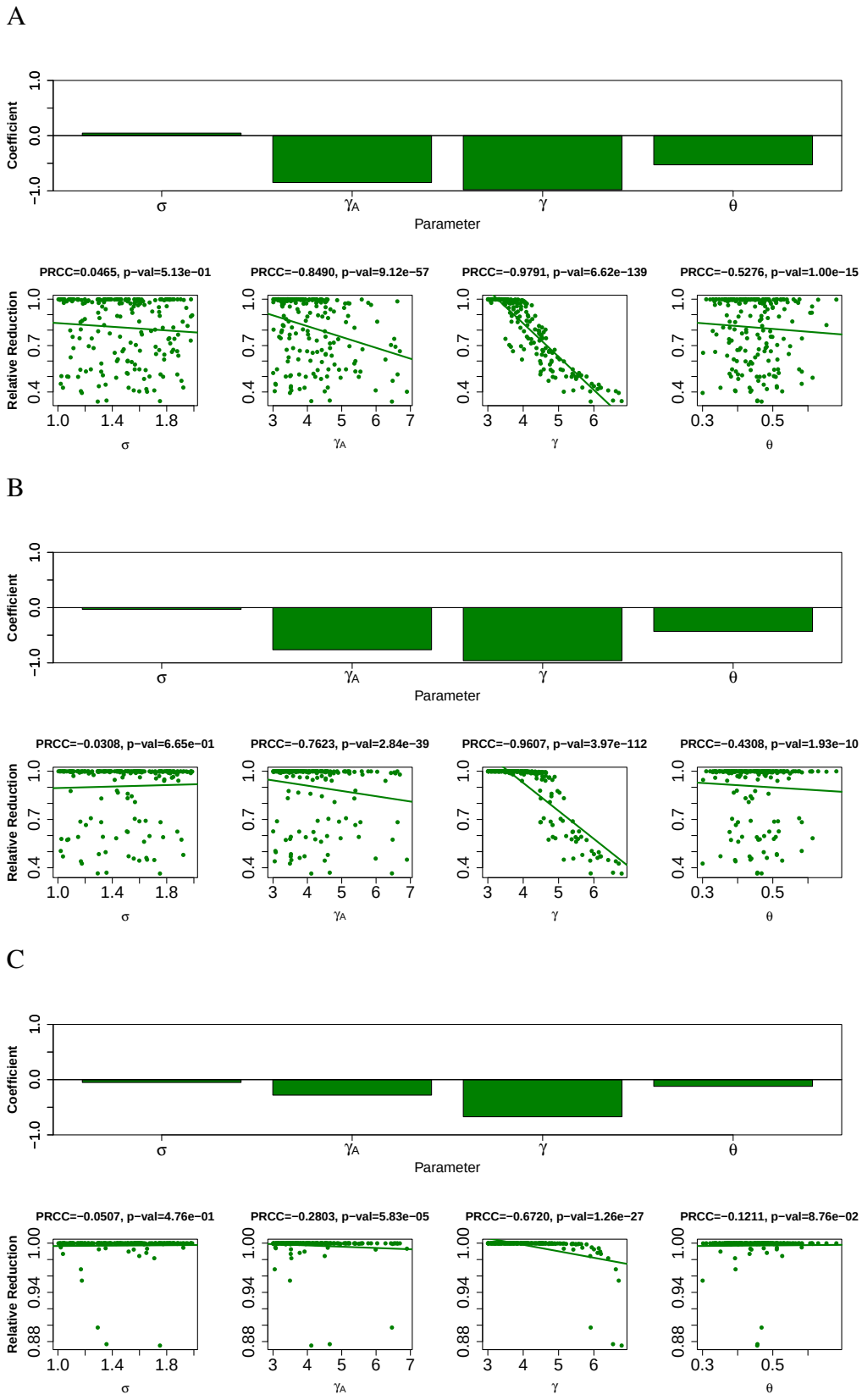

Figure 5.12: PRCC values with scatter plots for simulations using sampled parameters for influenza H1N1 with isolation (A), school closure (B) and lockdown (C) interventions.

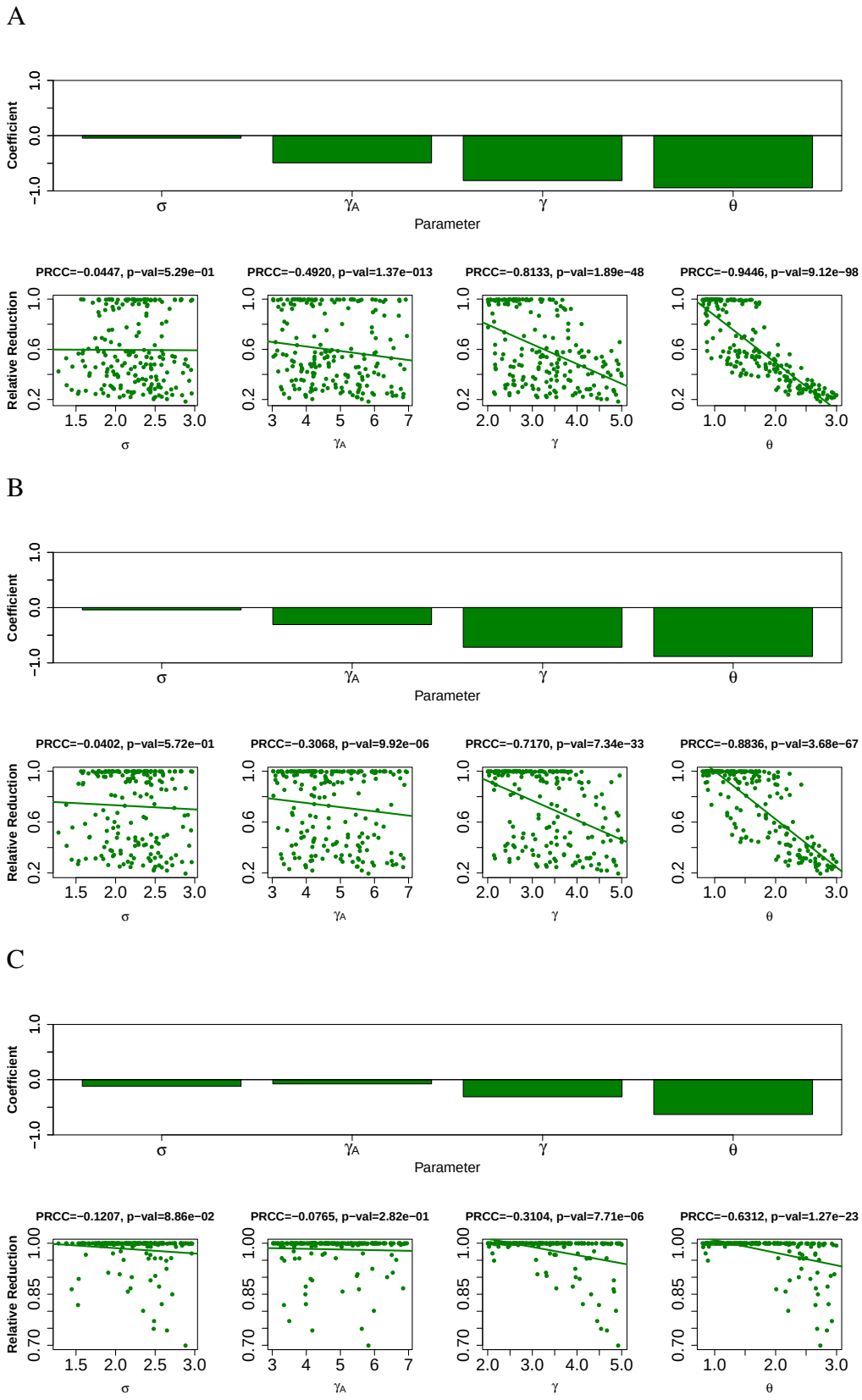

Figure 5.13: PRCC values with scatter plots for simulations using sampled parameters for SARS-CoV-2 original strain with isolation (A), school closure (B) and lockdown (C) interventions.

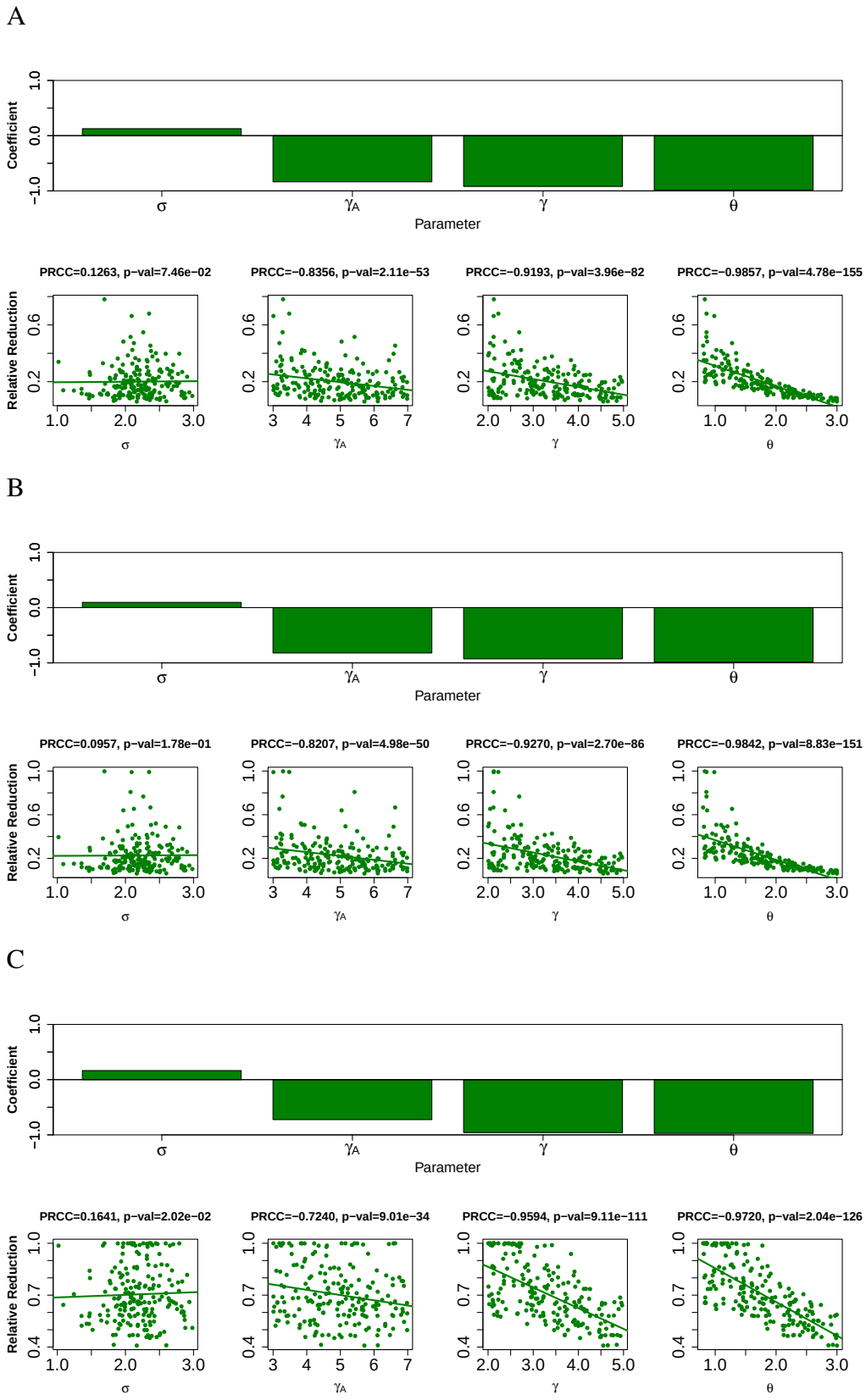

Figure 5.14: PRCC values with scatter plots for simulations using sampled parameters for SARS-CoV-2 Alpha variant with isolation (A), school closure (B) and lockdown (C) interventions.

the pre-symptomatic period, θ, and the RR in attack rate for all three scenarios isolation, school closure, and lockdown.

5.2.5 SARS-CoV-2: Omicron Variant

Finally, PRCCs were computed for SARS-CoV-2 Omicron variant (Figure 5.16). The result is nearly identical to that of the Delta variant. There are moderate negative, linear relationships between both the infectious period, γ, the pre-symptomatic period, θ, and the RR in attack rate for all three intervention scenarios of isolation, school closure, and lockdown.

5.3 Stochastic Simulations

We simulated the stochastic model to derive the overall daily and cumulative incidence, daily incidence by age, and attack rate for each intervention scenario using a Gillespie-like algorithm, in which the transition rates between model compartments were converted to the probability of its associated event. The baseline scenario (S1) without any interventions for influenza and the original strain of SARS-CoV-2 were calibrated to 55% attack rate in a totally susceptible population. The relative reduction (RR) in attack rate was calculated for interventions of isolation, school closure, and lockdown and were compared to the baseline for all viruses.

5.4 Influenza: H1N1

A transmission rate of $\beta = 0.0435$ was derived in the calibration of the baseline stochastic model. Using the fixed parameter values from Tables 4.3 and 4.5, Figure 5.17 illustrates the simulations for the overall incidence, cumulative incidence, age-based incidence, and attack rate. Due to a higher transmissibility compared to the determinsitic model (with the same baseline attack rate), the incidence peaks around 30 days (Figure Based on 5.17). In

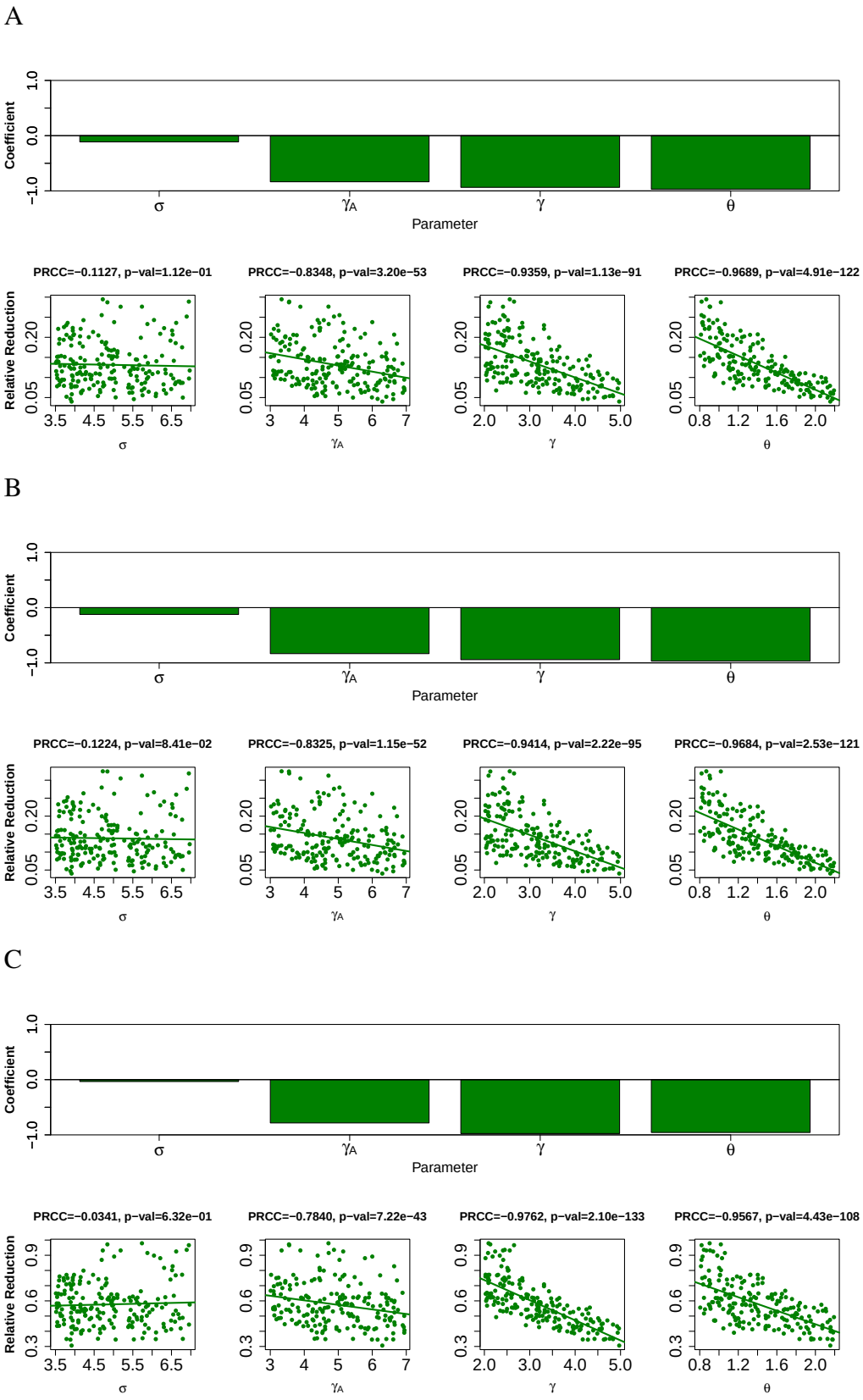

Figure 5.15: PRCC values with scatter plots for simulations using sampled parameters for SARS-CoV-2 Delta variant with isolation (A), school closure (B) and lockdown (C) interventions.

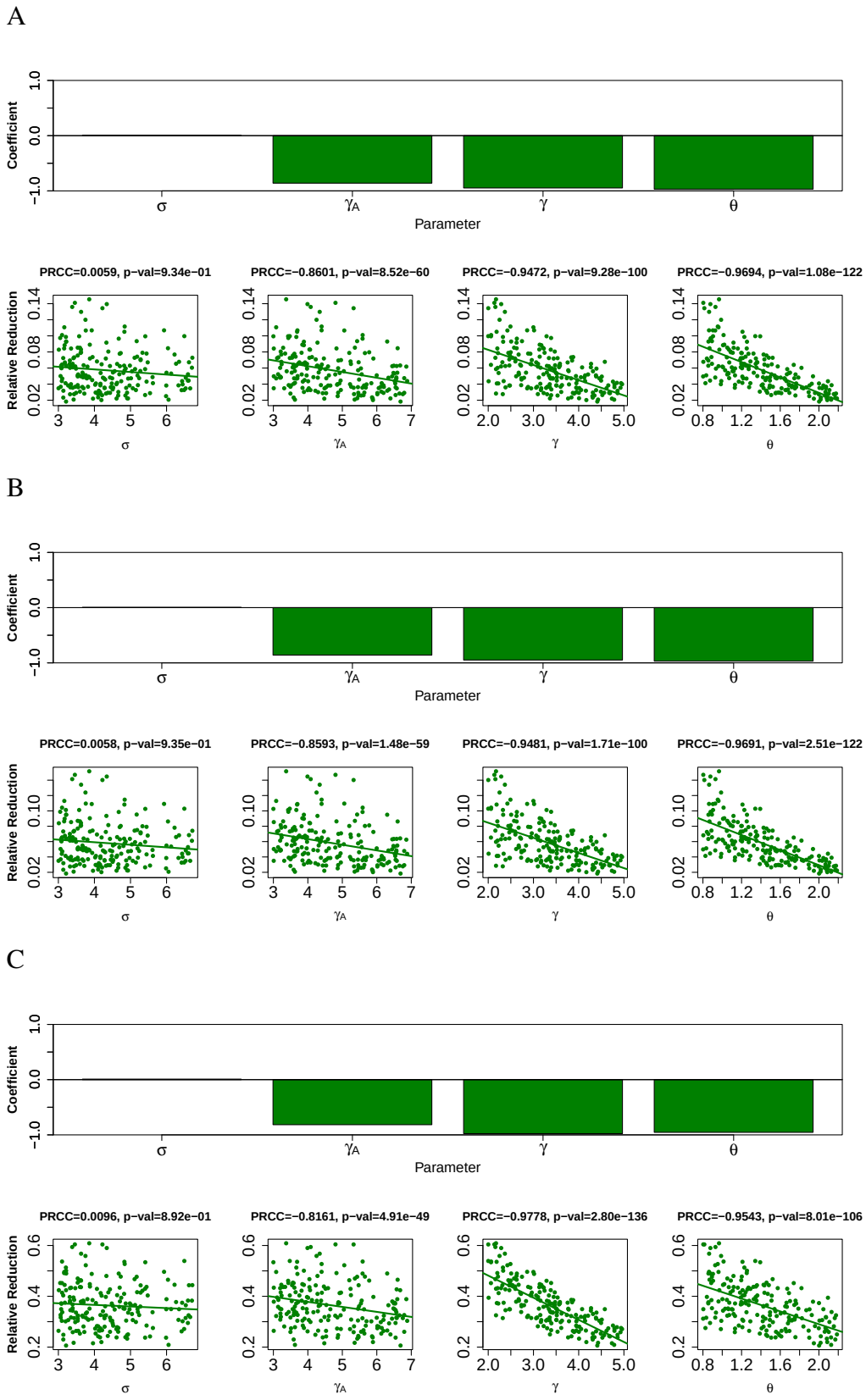

Figure 5.16: PRCC values with scatter plots for simulations using sampled parameters for SARS-CoV-2 Omicron variant with isolation (A), school closure (B) and lockdown (C) interventions.

the absence of interventions, the attack rate is highest in the 5–18 and 19–49 age groups.

5.5 SARS-CoV-2: Original Wuhan-I strain

For the SARS-CoV-2 original strain, the baseline transmission rate of $\beta = 0.033$ was derived in the stochastic model calibration. Based on the parameter values from Tables 4.3 and 4.5, Figure 5.18 illustrates the incidence (daily and cumulative) and attack rates. The peak incidence occurs later than what was displayed in Figure 5.17 around 50 days, likely due to the lower a transmissibility. The attack rate in the context of SARS-CoV-2 original strain is still highest among the socially active age groups 5–18 and 19–49 years old.

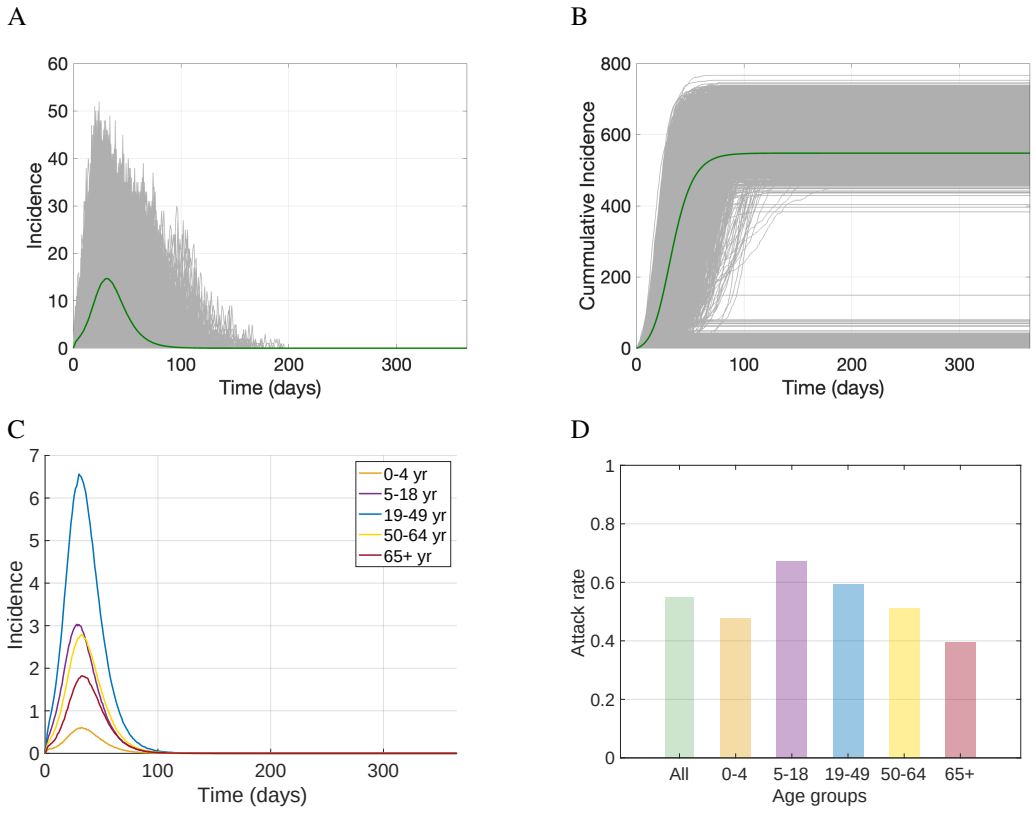

Figure 5.17: Stochastic simulations for influenza H1N1 without interventions representing daily incidence (A); cumulative incidence (B); age-stratified daily incidence (C); and age-stratified attack rates (D).

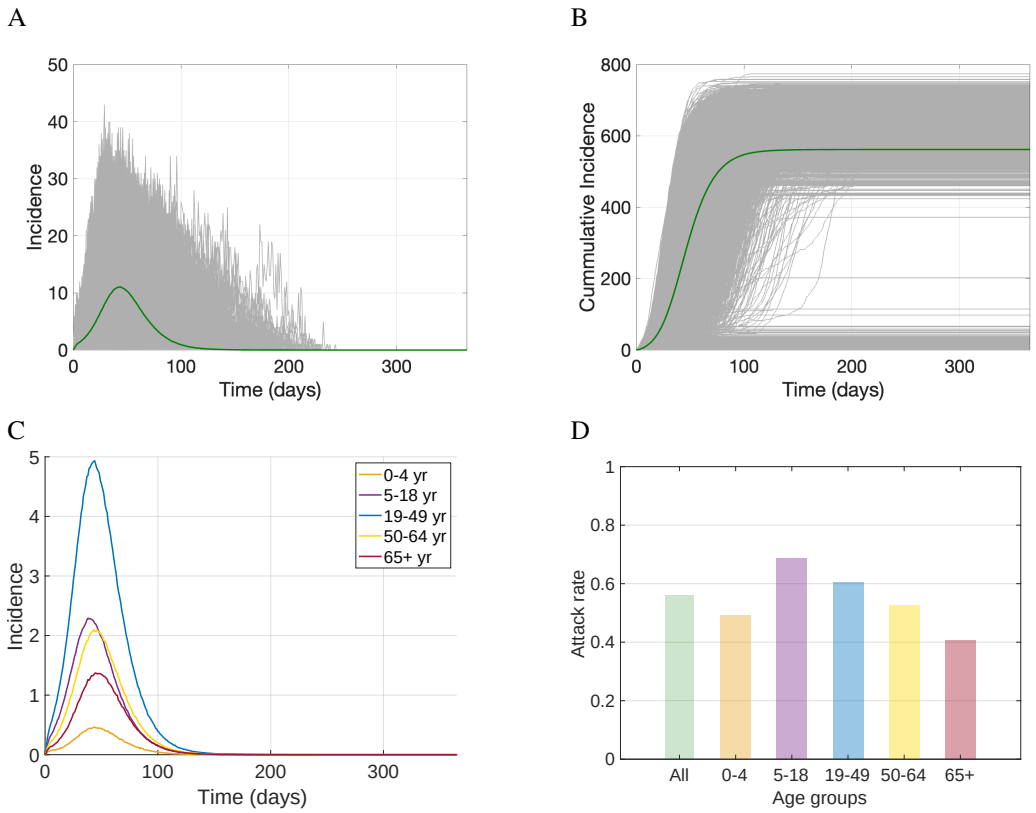

Figure 5.18: Stochastic simulations for SARS-CoV-2 original strain without interventions representing daily incidence (A); cumulative incidence (B); age-stratified daily incidence (C); and age-stratified attack rates (D).

5.6 SARS-CoV-2: Alpha Variant

For the Alpha variant, the baseline transmission rate of $\beta = 0.0495$ was derived, which is 50% higher than the original strain. using the fixed parameter values from Tables 4.3 and 4.5, Figure 5.19 illustrates the outcomes of simulations. With the increased transmissibility of this variant relative to the original strain, the peak incidence occurs earlier (Figure5.19), around 30 days. The attack rate increases substantially compared to that observed for the original strain, with all attack rates greater than 70% in all age groups without any intervention.

5.7 SARS-CoV-2: Delta Variant

For the Delta variant, the baseline transmission rate of $\beta = 0.06435$ was derived, being 30% higher than the Alpha variant. Based on the fixed parameters from Tables 4.3 and

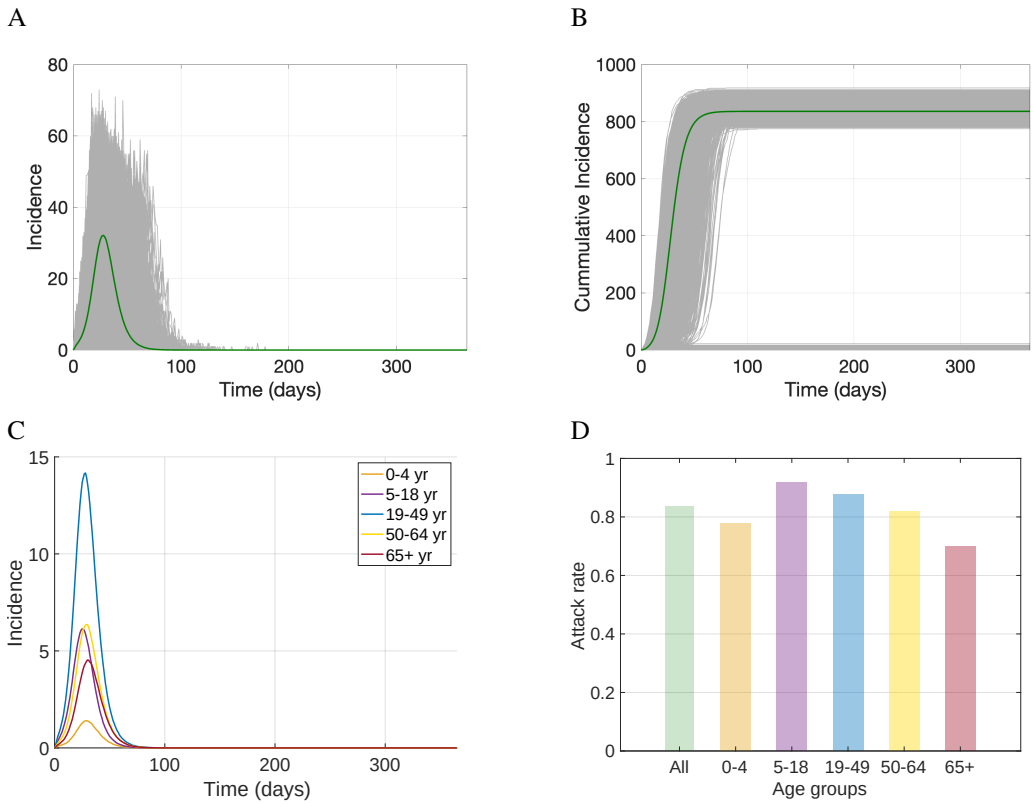

Figure 5.19: Stochastic simulations for SARS-CoV-2 Alpha variant without interventions representing daily incidence (A); cumulative incidence (B); age-stratified daily incidence (C); and age-stratified attack rates (D).

4.5, Figure 5.20 illustrates the daily and cumulative incidences, and the attack rate. Given its high transmissibility, the incidence peaks around the same time as the Alpha variant observed in Figure 5.19; however, the magnitude of incidence increases. The attack rate also increased compared to that observed for the Alpha variant, with all age-specific attack rates being 80% or greater.

5.8 SARS-CoV-2: Omicron Variant

Finally, for the most transmissible SARS-CoV-2 variant, Omicron, a baseline transmission rate of 35% higher than the Delta variant was assumed, giving $\beta = 0.08687$. Using the fixed parameters from Tables 4.3 and 4.5, Figure 5.21 illustrates that the incidence peaks rapidly around 20 days with comparatively highest attack rates of 90% and greater among all age groups.

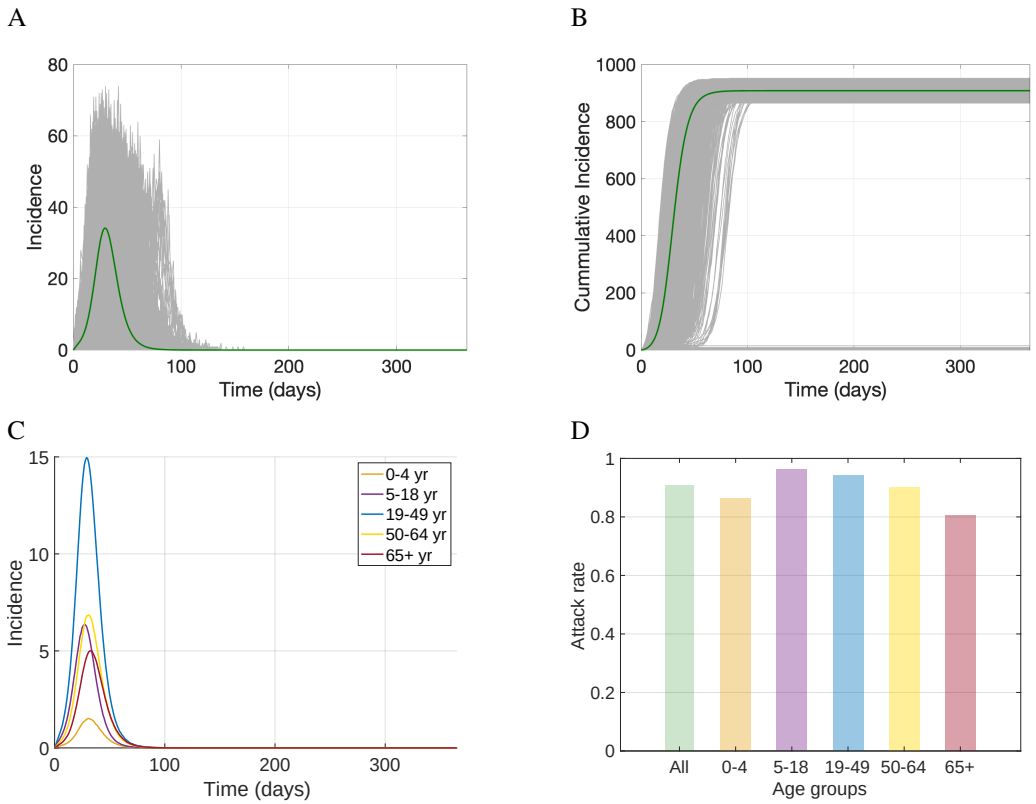

Figure 5.20: Stochastic simulations for SARS-CoV-2 Delta variant without interventions representing daily incidence (A); cumulative incidence (B); age-stratified daily incidence (C); and age-stratified attack rates (D).

5.9 Relative Reduction (RR) in Attack Rate

The RR in attack rate was computed in a similar manner to that of the deterministic model for the interventions of isolation, school closure, and lockdown, considering the baseline of no interventions as the reference with the fixed parameters from Tables 4.3 and 4.5. Similar to the deterministic model, the RR increases as stricter interventions are implemented (Figure 5.22); however, the overall and age-specific RRs are lower than those observed in the deterministic model. For example, the RR reaches approximately 90% when lockdown was implemented in the stochastic model for influenza, while it nearly eliminated the disease in the deterministic model. Overall, each intervention had the greatest impact on influenza, with comparatively decreasing effects on variants of SARS-CoV-2 as the transmissibility increased. In general, this was observed in the deterministic simulations as well, however, the effects are less pronounced in the stochastic simulations. The lowest impact was observed on the Omicron variant. Comparing the RRs in Figure

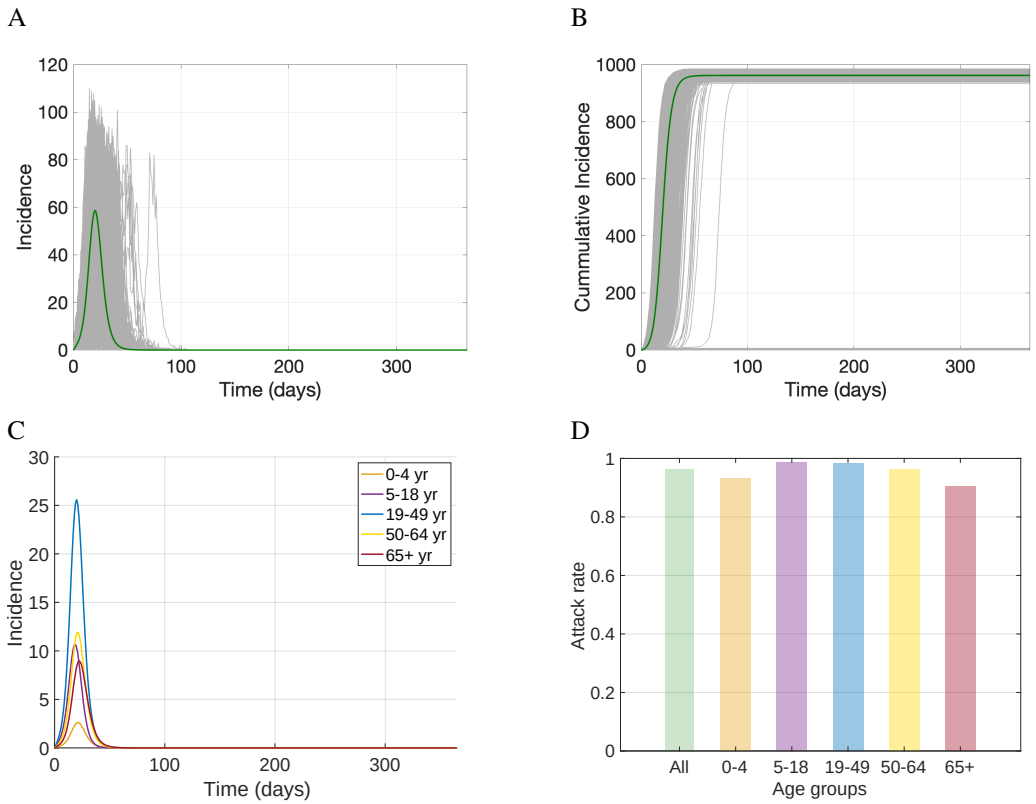

Figure 5.21: Stochastic simulations for SARS-CoV-2 Omicron variant without interventions representing daily incidence (A); cumulative incidence (B); age-stratified daily incidence (C); and age-stratified attack rates (D).

5.22A and 5.22B, it is evident that the intervention of school closure has the largest impact on children 5–18 years old with approximately 2-fold increase compared to isolation only. However, the increase in RR among other age groups is significantly lower. Compared to influenza, the overall and age-specific RR for all variants of SARS-CoV-2 are lower. The results presented here imply that isolation as a single intervention is more effective than school closure for a disease with similar characteristics to SARS-CoV-2 compared to influenza. As expected, a lockdown results in the highest RR in attack rate for all scenarios, however, the impact is lower for SARS-CoV-2 original strain and its variants compared to influenza.

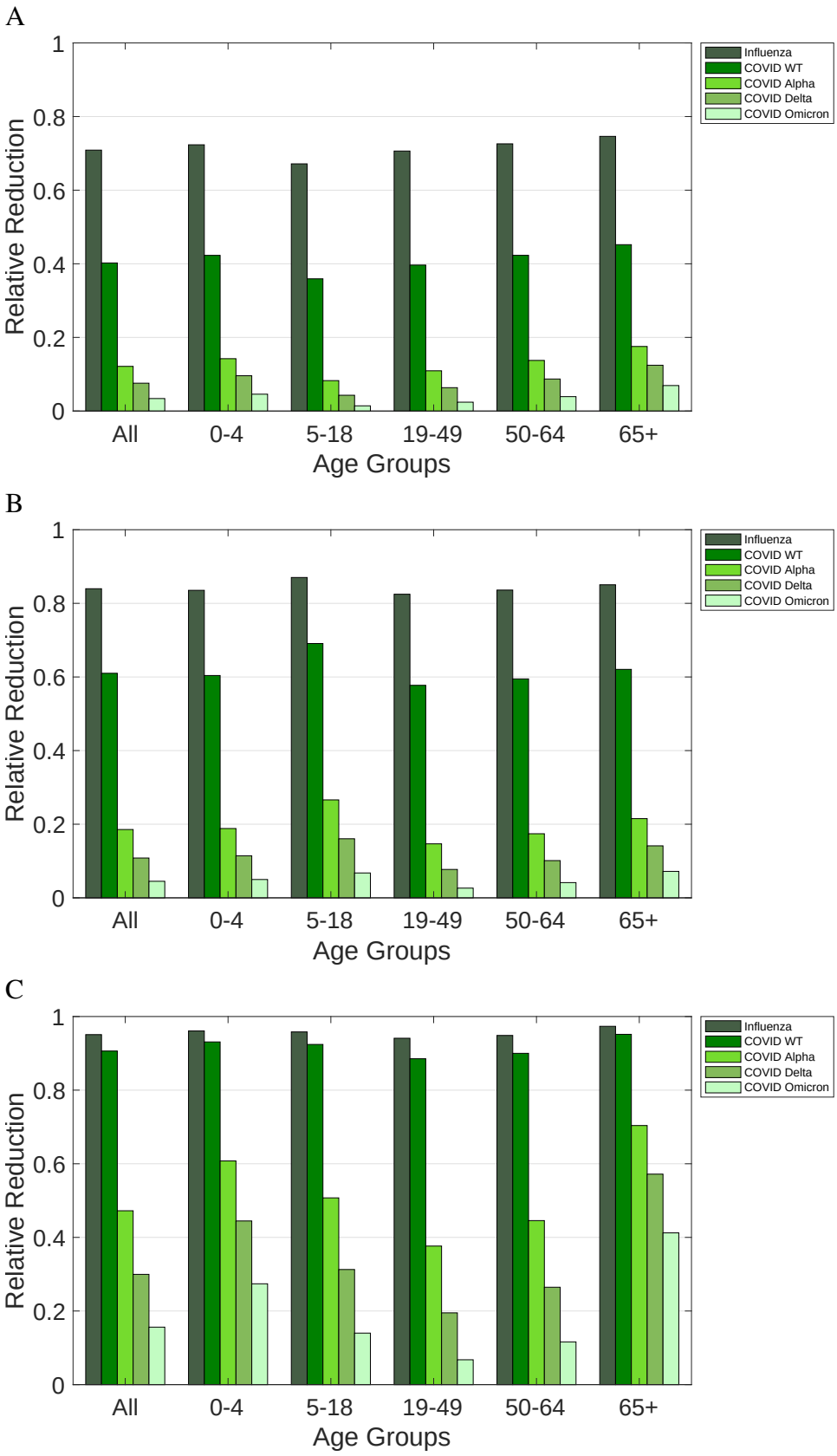

Figure 5.22: Relative reduction of the overall and age-specific attack rates achieved for influenza and variants of SARS-CoV-2 with different interventions of isolation (A); school closure (B), and lockdown (C).

Chapter 6

Discussion

Exploring the interplay between disease characteristics and intervention outcomes is an important step towards developing effective public health policies and interventions to combat emerging infectious diseases. Understanding how these characteristics differ between diseases, for example influenza and SARS-CoV-2 variants is essential to ensure the utilization of strategies that have the maximum impact on preventing future epidemics or pandemics, and reducing the socioeconomic consequences. The objective of this thesis was to understand the effect of these characteristics in the presence of several interventions that were implemented during the COVID-19 pandemic. This work is useful in highlighting optimal interventions based on the disease in question and quantifying the effect of type and intensity of interventions.

The results indicate that the effect and potency of intervention measures depend immensely on the characteristics of a given disease. It is clear that increasing the severity of interventions (i.e. isolation, to school closure, to lockdown) has an impact on all diseases, especially in the event of a lockdown. We observe a more flattened curve as more strict interventions are implemented, however; it is clear that the impact of each intervention is different between influenza and SARS-CoV-2.

A key result from both the deterministic and stochastic simulations is the differences in the impact on influenza and SARS-CoV-2 when using a school closure. This type of

intervention has proven to prevent transmission in the population through young children, but its effect is minimal for a disease such as SARS-CoV-2. The implication is that when we consider a disease which has a longer and more transmissible pre-symptomatic period, age-specific interventions (like school closure) may have limited effects on curbing the transmission dynamics. Furthermore, it is evident that the length of the symptomatic period and infectiousness during the symptomatic period has a remarkable influence on the outcome of interventions. The difference in school closure outcomes between influenza and SARS-CoV-2 may be due to the differences in their respective infectiousness profiles and duration of the pre-symptomatic and symptomatic periods. This idea is further established by the results from the sensitivity analysis, which showed that the pre-symptomatic and symptomatic periods consistently exhibit a negative linear relationship with the RR in attack rate, regardless of the disease or intervention. Overall, the simulation results from both the deterministic and stochastic models indicate that isolation as a single measure has a greater effect on reducing disease incidence than school closure alone (without isolation).

6.1 Limitations

This study has several limitations that merit further research. Despite including age groups and using age-specific contact patterns derived from data collected during the COVID-19 pandemic, the model is homogeneous by nature; and does not include many factors that could affect disease dynamics and intervention outcomes. Additionally, we used parameters values and distributions associated with the diseases natural history; however, sampled parameters were applied at the population level for simulating the model. Realistically, sampling should be conducted at the individual level; a feature that is not attainable under the compartmental modelling structure employed in this work. For example, the incubation, pre-symptomatic, and infectious periods may be different between individuals. Naturally, an extension of this structure to an agent-based

model would allow for the inclusion of various heterogeneities and individual-level sampling from distributions. Furthermore, the effect of interventions were captured in contact patterns without taking into consideration other important factors, such as measures that may be mandated by public health during a lockdown. As well, intervention scenarios were evaluated in the context of a fully susceptible population. If the population has pre-existing immunity (due to prior infection or vaccination), the effect of these interventions may be altered depending on the level of population immunity in different age groups. Interventions were assumed to be implemented at the start of simulation after the introduction of the disease into the population, which may not be completely realistic. Interventions are usually implemented once some threshold of infection in the population is reached. However, the timing of interventions does not affect the comparative results in terms of the relative reduction of attack rates. Finally, we assumed that recovery from infection provides relatively long protection, and thus omitted re-infection in the model. However, as we have seen during the COVID-19 pandemic, re-infection with the same or different variants can occur. To further investigate the effects of immunity on intervention outcomes, the general modelling framework which includes waning immunity and re-infection should be analyzed.

Although our results highlight the importance of disease characteristics on intervention outcomes, there are various factors that could simultaneously influence interventions such behavioural responses, the health status of individuals, and immunity in the population, which are not considered in our model and require more comprehensive (e.g., agent-based) models. Addressing these limitations remain a future task beyond the scope of this thesis.

Bibliography

[1] Seyed M. Moghadas. "Gaining insights into human viral diseases through mathematics". In: *European Journal of Epidemiology* 21.5 (2006), pp. 337–342. ISSN: 0393-2990, 1573-7284. DOI: 10.1007/s10654-006-9007-z. URL: http://link.springer.com/10.1007/s10654-006-9007-z.

[2] Seyed M. Moghadas et al. "The implications of silent transmission for the control of COVID-19 outbreaks". In: *Proceedings of the National Academy of Sciences* 117.30 (28, 2020), pp. 17513–17515. ISSN: 0027-8424, 1091-6490. DOI: 10.1073/pnas.2008373117. URL: https://pnas.org/doi/full/10.1073/pnas.2008373117.

[3] Rachael Milwid et al. "Toward Standardizing a Lexicon of Infectious Disease Modeling Terms". In: *Frontiers in Public Health* 4 (28, 2016). ISSN: 2296-2565. DOI: 10.3389/fpubh.2016.00213. URL: http://journal.frontiersin.org/Article/10.3389/fpubh.2016.00213/abstract.

[4] World Health Organization Writing Group. "Nonpharmaceutical Interventions for Pandemic Influenza, International Measures". In: *Emerging Infectious Diseases* 12.1 (2006), pp. 81–87. ISSN: 1080-6040, 1080-6059. DOI: 10.3201/eid1201.051370. URL: http://wwwnc.cdc.gov/eid/article/12/1/05-1370_article.htm.

[5] Harpa K. Isfeld-Kiely and Seyed Moghadas. *Effectiveness of school closure for the control of influenza: a review of recent evidence*. Winnipeg, Manitoba: National Collaborating Centre for Infectious Diseases, 2014. ISBN: 978-1-927988-14-5.

[6] Elaheh Abdollahi et al. “Simulating the effect of school closure during COVID-19 outbreaks in Ontario, Canada”. In: *BMC Medicine* 18.1 (2020), p. 230. ISSN: 1741-7015. DOI: 10.1186/s12916-020-01705-8. URL: https://bmcmedicine.biomedcentral.com/articles/10.1186/s12916-020-01705-8.

[7] Joseph T Wu et al. “A global assessment of the impact of school closure in reducing COVID- spread”. In: *.j.o.u.rn. a. .l* (), p. 17.

[8] Dan Yamin et al. “Effect of Ebola Progression on Transmission and Control in Liberia”. In: *Annals of Internal Medicine* 162.1 (6, 2015), pp. 11–17. ISSN: 0003-4819, 1539-3704. DOI: 10.7326/M14-2255. URL: https://www.acpjournals.org/doi/10.7326/M14-2255.

[9] Edward Burn et al. “The natural history of symptomatic COVID-19 during the first wave in Catalonia”. In: *Nature Communications* 12.1 (2021), p. 777. ISSN: 2041-1723. DOI: 10.1038/s41467-021-21100-y. URL: http://www.nature.com/articles/s41467-021-21100-y.

[10] Michael A. Johansson et al. “SARS-CoV-2 Transmission From People Without COVID-19 Symptoms”. In: *JAMA Network Open* 4.1 (7, 2021), e2035057. ISSN: 2574-3805. DOI: 10.1001/jamanetworkopen.2020.35057. URL: https://jamanetwork.com/journals/jamanetworkopen/fullarticle/2774707.

[11] Moira A. Mugglestone et al. “Presymptomatic, asymptomatic and post-symptomatic transmission of SARS-CoV-2: joint British Infection Association (BIA), Healthcare Infection Society (HIS), Infection Prevention Society (IPS) and Royal College of Pathologists (RCPath) guidance”. In: *BMC Infectious Diseases* 22.1 (2022), p. 453. ISSN: 1471-2334. DOI: 10.1186/s12879-022-07440-0. URL: https://bmcinfectdis.biomedcentral.com/articles/10.1186/s12879-022-07440-0.

[12] Christina Savvides and Robert Siegel. *Asymptomatic and presymptomatic transmission of SARS-CoV-2: A systematic review*. preprint. Epidemiology, 14, 2020. DOI:

10.1101/2020.06.11.20129072. URL: http://medrxiv.org/lookup/doi/10.1101/2020.06.11.20129072.

[13] Monica Gandhi. "Asymptomatic Transmission, the Achilles Heel of Current Strategies to Control Covid-19". In: *n engl j med* (2020), p. 3.

[14] Xi He et al. "Temporal dynamics in viral shedding and transmissibility of COVID-19". In: *Nature Medicine* 26.5 (1, 2020), pp. 672–675. ISSN: 1078-8956, 1546-170X. DOI: 10.1038/s41591-020-0869-5. URL: http://www.nature.com/articles/s41591-020-0869-5.

[15] William S Hart, Philip K Maini, and Robin N Thompson. "High infectiousness immediately before COVID-19 symptom onset highlights the importance of continued contact tracing". In: *eLife* 10 (26, 2021), e65534. ISSN: 2050-084X. DOI: 10.7554/eLife.65534. URL: https://elifesciences.org/articles/65534.

[16] C.W. Potter. "A history of influenza". In: *Journal of Applied Microbiology* 91.4 (2001), pp. 572–579. ISSN: 1364-5072, 1365-2672. DOI: 10.1046/j.1365-2672.2001.01492.x. URL: http://doi.wiley.com/10.1046/j.1365-2672.2001.01492.x.

[17] Jeffery K Taubenberger and David M Morens. "1918 Influenza: the Mother of All Pandemics". In: *Emerging Infectious Diseases* 12.1 (2006).

[18] cdc_1918. *1918 Pandemic Influenza Historic Timeline | Pandemic Influenza (Flu) | CDC*. 18, 2019. URL: https://www.cdc.gov/flu/pandemic-resources/1918-commemoration/pandemic-timeline-1918.htm.

[19] Peter Spreeuwenberg, Madelon Kroneman, and John Paget. "Reassessing the Global Mortality Burden of the 1918 Influenza Pandemic". In: *American Journal of Epidemiology* 187.12 (1, 2018), pp. 2561–2567. ISSN: 0002-9262, 1476-6256. DOI: 10.1093/aje/kwy191. URL: https://academic.oup.com/aje/article/187/12/2561/5092383.

[20] Christina E. Mills, James M. Robins, and Marc Lipsitch. "Transmissibility of 1918 pandemic influenza". In: *Nature* 432.7019 (2004), pp. 904–906. ISSN: 0028-0836, 1476-4687. DOI: 10.1038/nature03063. URL: http://www.nature.com/articles/nature03063.

[21] stacey knobler stacey. *The Threat of Pandemic Influenza: Are We Ready? Workshop Summary*. Washington, D.C.: National Academies Press, 9, 2005. ISBN: 978-0-309-09504-4. DOI: 10.17226/11150. URL: http://www.nap.edu/catalog/11150.

[22] Thomas N. Vilches, Majid Jaberi-Douraki, and Seyed M. Moghadas. "Risk of influenza infection with low vaccine effectiveness: the role of avoidance behaviour". In: *Epidemiology and Infection* 147 (2019), e75. ISSN: 0950-2688, 1469-4409. DOI: 10.1017/S0950268818003540. URL: https://www.cambridge.org/core/product/identifier/S0950268818003540/type/journal_article.

[23] Diana Duong. "Alpha, Beta, Delta, Gamma: Whats important to know about SARS-CoV-2 variants of concern?" In: *Canadian Medical Association Journal* 193.27 (12, 2021), E1059–E1060. ISSN: 0820-3946, 1488-2329. DOI: 10.1503/cmaj.1095949. URL: http://www.cmaj.ca/lookup/doi/10.1503/cmaj.1095949.

[24] Finlay Campbell et al. "Increased transmissibility and global spread of SARS-CoV-2 variants of concern as at June 2021". In: *Eurosurveillance* 26.24 (17, 2021). ISSN: 1560-7917. DOI: 10.2807/1560-7917.ES.2021.26.24.2100509. URL: https://www.eurosurveillance.org/content/10.2807/1560-7917.ES.2021.26.24.2100509.

[25] Nicholas G. Davies et al. "Estimated transmissibility and impact of SARS-CoV-2 lineage B.1.1.7 in England". In: *Science* 372.6538 (9, 2021), eabg3055. ISSN: 0036-8075, 1095-9203. DOI: 10.1126/science.abg3055. URL: https://www.science.org/doi/10.1126/science.abg3055.

[26] CMMID COVID-19 Working Group et al. “Increased mortality in community-tested cases of SARS-CoV-2 lineage B.1.1.7”. In: *Nature* 593.7858 (13, 2021), pp. 270–274. ISSN: 0028-0836, 1476-4687. DOI: 10.1038/s41586-021-03426-1. URL: http://www.nature.com/articles/s41586-021-03426-1.

[27] Ying Liu and Joacim Rocklöv. “The reproductive number of the Delta variant of SARS-CoV-2 is far higher compared to the ancestral SARS-CoV-2 virus”. In: *Journal of Travel Medicine* 28.7 (11, 2021), taab124. ISSN: 1195-1982, 1708-8305. DOI: 10.1093/jtm/taab124. URL: https://academic.oup.com/jtm/article/doi/10.1093/jtm/taab124/6346388.

[28] Hester Allen et al. “Household transmission of COVID-19 cases associated with SARS-CoV-2 delta variant (B.1.617.2): national case-control study”. In: *The Lancet Regional Health - Europe* 12 (2022), p. 100252. ISSN: 26667762. DOI: 10.1016/j.lanepe.2021.100252. URL: https://linkinghub.elsevier.com/retrieve/pii/S2666776221002386.

[29] Mahesh S. Dhar et al. “Genomic characterization and epidemiology of an emerging SARS-CoV-2 variant in Delhi, India”. In: *Science* 374.6570 (19, 2021), pp. 995–999. ISSN: 0036-8075, 1095-9203. DOI: 10.1126/science.abj9932. URL: https://www.science.org/doi/10.1126/science.abj9932.

[30] Yu-Dong Zhang et al. “Epidemiological Characteristics of COVID-19 Outbreak in Yangzhou, China, 2021”. In: *Frontiers in Microbiology* 13 (6, 2022), p. 865963. ISSN: 1664-302X. DOI: 10.3389/fmicb.2022.865963. URL: https://www.frontiersin.org/articles/10.3389/fmicb.2022.865963/full.

[31] Nuno R. Faria et al. “Genomics and epidemiology of the P.1 SARS-CoV-2 lineage in Manaus, Brazil”. In: *Science* 372.6544 (21, 2021), pp. 815–821. ISSN: 0036-8075, 1095-9203. DOI: 10.1126/science.abh2644. URL: https://www.science.org/doi/10.1126/science.abh2644.

[32] Chad R. Wells et al. “Optimal COVID-19 quarantine and testing strategies”. In: *Nature Communications* 12.1 (7, 2021), p. 356. ISSN: 2041-1723. DOI: 10.1038/s41467-020-20742-8. URL: https://www.nature.com/articles/s41467-020-20742-8.

[33] Chad R. Wells et al. “Quarantine and testing strategies to ameliorate transmission due to travel during the COVID-19 pandemic: a modelling study”. In: *The Lancet Regional Health - Europe* 14 (2022). ISSN: 26667762. DOI: 10.1016/j.lanepe.2021.100304. URL: https://linkinghub.elsevier.com/retrieve/pii/S2666776221002908.

[34] Chad R Wells et al. “Quarantine and serial testing for variants of SARS-CoV-2 with benefits of vaccination and boosting on consequent control of COVID-19”. In: *PNAS Nexus* 1.3 (1, 2022). Ed. by Karen E Nelson, pgac100. ISSN: 2752-6542. DOI: 10.1093/pnasnexus/pgac100. URL: https://academic.oup.com/pnasnexus/article/doi/10.1093/pnasnexus/pgac100/6650682.

[35] Helen Onyeaka et al. “COVID-19 pandemic: A review of the global lockdown and its far-reaching effects”. In: *Science Progress* 104.2 (2021), p. 003685042110198. ISSN: 0036-8504, 2047-7163. DOI: 10.1177/00368504211019854. URL: http://journals.sagepub.com/doi/10.1177/00368504211019854.

[36] Laura Di Domenico et al. “Impact of lockdown on COVID-19 epidemic in Île-de-France and possible exit strategies”. In: *BMC Medicine* 18.1 (2020), p. 240. ISSN: 1741-7015. DOI: 10.1186/s12916-020-01698-4. URL: https://bmcmedicine.biomedcentral.com/articles/10.1186/s12916-020-01698-4.

[37] Vincenzo Alfano and Salvatore Ercolano. “The Efficacy of Lockdown Against COVID-19: A Cross-Country Panel Analysis”. In: *Applied Health Economics and Health Policy* 18.4 (2020), pp. 509–517. ISSN: 1175-5652, 1179-1896. DOI:

10.1007/s40258-020-00596-3. URL: https://link.springer.com/10.1007/s40258-020-00596-3.

[38] Matthew Biggerstaff et al. "Estimates of the reproduction number for seasonal, pandemic, and zoonotic influenza: a systematic review of the literature". In: *BMC Infectious Diseases* 14.1 (2014), p. 480. ISSN: 1471-2334. DOI: 10.1186/1471-2334-14-480. URL: https://bmcinfectdis.biomedcentral.com/articles/10.1186/1471-2334-14-480.

[39] A. Cori et al. "Estimating influenza latency and infectious period durations using viral excretion data". In: *Epidemics* 4.3 (2012), pp. 132–138. ISSN: 17554365. DOI: 10.1016/j.epidem.2012.06.001. URL: https://linkinghub.elsevier.com/retrieve/pii/S175543651200031X.

[40] Justin Lessler et al. "Incubation periods of acute respiratory viral infections: a systematic review". In: *The Lancet Infectious Diseases* 9.5 (2009), pp. 291–300. ISSN: 14733099. DOI: 10.1016/S1473-3099(09)70069-6. URL: https://linkinghub.elsevier.com/retrieve/pii/S1473309909700696.

[41] Christopher W Woods et al. "A Host Transcriptional Signature for Presymptomatic Detection of Infection in Humans Exposed to Influenza H1N1 or H3N2". In: *PLOS ONE* 8.1 (2013), p. 9.

[42] G. F. Webb et al. "Pre-symptomatic Influenza Transmission, Surveillance, and School Closings: Implications for Novel Influenza A (H1N1)". In: *Mathematical Modelling of Natural Phenomena* 5.3 (2010), pp. 191–205. ISSN: 0973-5348, 1760-6101. DOI: 10.1051/mmnp/20105312. URL: http://www.mmnp-journal.org/10.1051/mmnp/20105312.

[43] Nancy H. L. Leung. "Transmissibility and transmission of respiratory viruses". In: *Nature Reviews Microbiology* 19.8 (2021), pp. 528–545. ISSN: 1740-1526, 1740-1534. DOI: 10.1038/s41579-021-00535-6. URL: http://www.nature.com/articles/s41579-021-00535-6.

[44] Eleni Patrozou and Leonard A. Mermel. "Does Influenza Transmission Occur from Asymptomatic Infection or Prior to Symptom Onset?" In: *Public Health Reports* 124.2 (2009), pp. 193–196. ISSN: 0033-3549, 1468-2877. DOI: 10.1177/003335490912400205. URL: http://journals.sagepub.com/doi/10.1177/003335490912400205.

[45] Cheryl Cohen et al. "Asymptomatic transmission and high community burden of seasonal influenza in an urban and a rural community in South Africa, 201718 (PHIRST): a population cohort study". In: *The Lancet Global Health* 9.6 (2021), e863–e874. ISSN: 2214109X. DOI: 10.1016/S2214-109X(21)00141-8. URL: https://linkinghub.elsevier.com/retrieve/pii/S2214109X21001418.

[46] Nicholas H Ogden et al. "Counterfactuals of effects of vaccination and public health measures on COVID-19 cases in Canada: What could have happened?" In: *Canada Communicable Disease Report* 48.7 (3, 2022), pp. 292–302. ISSN: 14818531. DOI: 10.14745/ccdr.v48i78a01. URL: https://www.canada.ca/en/public-health/services/reports-publications/canada-communicable-disease-report-ccdr/monthly-issue/2022-48/issue-7-8-july-august-2022/counterfactuals-effects-vaccination-public-health-measures-covid-19-cases-canada.html.

[47] Ruiyun Li et al. "Substantial undocumented infection facilitates the rapid dissemination of novel coronavirus (SARS-CoV-2)". In: *Science* 368.6490 (2020), pp. 489–493. ISSN: 0036-8075, 1095-9203. DOI: 10.1126/science.abb3221. URL: https://www.science.org/doi/10.1126/science.abb3221.

[48] Stephen A. Lauer et al. "The Incubation Period of Coronavirus Disease 2019 (COVID-19) From Publicly Reported Confirmed Cases: Estimation and Application". In: *Annals of Internal Medicine* 172.9 (5, 2020), pp. 577–582. ISSN: 0003-4819, 1539-3704. DOI: 10.7326/M20-0504. URL: https://www.acpjournals.org/doi/10.7326/M20-0504.

[49] Yutong Wang et al. “Asymptomatic and pre-symptomatic infection in Coronavirus Disease 2019 pandemic”. In: *Medical Review* 2.1 (23, 2022), pp. 66–88. ISSN: 2749-9642. DOI: 10.1515/mr-2021-0034. URL: https://www.degruyter.com/document/doi/10.1515/mr-2021-0034/html.

[50] Pratha Sah et al. “Asymptomatic SARS-CoV-2 infection: A systematic review and meta-analysis”. In: *Proceedings of the National Academy of Sciences* 118.34 (24, 2021), e2109229118. ISSN: 0027-8424, 1091-6490. DOI: 10.1073/pnas.2109229118. URL: https://pnas.org/doi/full/10.1073/pnas.2109229118.

[51] Zhanwei Du et al. “Reproduction Numbers of Severe Acute Respiratory Syndrome Coronavirus 2 (SARS-CoV-2) Variants: A Systematic Review and Meta-analysis”. In: *Clinical Infectious Diseases* (16, 2022), ciac137. ISSN: 1058-4838, 1537-6591. DOI: 10.1093/cid/ciac137. URL: https://academic.oup.com/cid/advance-article/doi/10.1093/cid/ciac137/6529536.

[52] Yu Wu et al. “Incubation Period of COVID-19 Caused by Unique SARS-CoV-2 Strains: A Systematic Review and Meta-analysis”. In: *JAMA Network Open* 5.8 (22, 2022), e2228008. ISSN: 2574-3805. DOI: 10.1001/jamanetworkopen.2022.28008. URL: https://jamanetwork.com/journals/jamanetworkopen/fullarticle/2795489.

[53] Sam Li-Sheng Chen et al. *A New Approach to Modelling Pre-symptomatic Incidence and Transmission Time of SARS-CoV-2 Variants*. preprint. In Review, 3, 2022. DOI: 10.21203/rs.3.rs-1561446/v1. URL: https://www.researchsquare.com/article/rs-1561446/v1.

[54] Terry C. Jones et al. “Estimating infectiousness throughout SARS-CoV-2 infection course”. In: *Science* 373.6551 (9, 2021), eabi5273. ISSN: 0036-8075, 1095-9203. DOI: 10.1126/science.abi5273. URL: https://www.science.org/doi/10.1126/science.abi5273.

[55] Hui Xu et al. “Demographic, Virological Characteristics and Prognosis of Asymptomatic COVID-19 Patients in South China”. In: *Frontiers in Medicine* 9 (28, 2022), p. 830942. ISSN: 2296-858X. DOI: 10.3389/fmed.2022.830942. URL: https://www.frontiersin.org/articles/10.3389/fmed.2022.830942/full.

[56] Andrew William Byrne et al. “Inferred duration of infectious period of SARS-CoV-2: rapid scoping review and analysis of available evidence for asymptomatic and symptomatic COVID-19 cases”. In: *BMJ Open* 10.8 (2020), e039856. ISSN: 2044-6055, 2044-6055. DOI: 10.1136/bmjopen-2020-039856. URL: https://bmjopen.bmj.com/lookup/doi/10.1136/bmjopen-2020-039856.

[57] Minami Ueda, Tetsuro Kobayashi, and Hiroshi Nishiura. “Basic reproduction number of the COVID-19 Delta variant: Estimation from multiple transmission datasets”. In: *Mathematical Biosciences and Engineering* 19.12 (2022), pp. 13137–13151. ISSN: 1551-0018. DOI: 10.3934/mbe.2022614. URL: http://www.aimspress.com/article/doi/10.3934/mbe.2022614.

[58] Cristina Menni et al. “Symptom prevalence, duration, and risk of hospital admission in individuals infected with SARS-CoV-2 during periods of omicron and delta variant dominance: a prospective observational study from the ZOE COVID Study”. In: *The Lancet* 399.10335 (2022), pp. 1618–1624. ISSN: 01406736. DOI: 10.1016/S0140-6736(22)00327-0. URL: https://linkinghub.elsevier.com/retrieve/pii/S0140673622003270.

[59] Weien Yu et al. “Proportion of asymptomatic infection and nonsevere disease caused by SARS8208;CoV8208;2 Omicron variant: A systematic review and analysis”. In: *Journal of Medical Virology* (24, 2022), jmv.28066. ISSN: 0146-6615, 1096-9071. DOI: 10.1002/jmv.28066. URL: https://onlinelibrary.wiley.com/doi/10.1002/jmv.28066.

[60] Tsuyoshi Ogata et al. “A low proportion of asymptomatic COVID-19 patients with the Delta variant infection by viral transmission through household contact at the

time of confirmation in Ibaraki, Japan". In: *Global Health & Medicine* 4.3 (30, 2022), pp. 192–196. ISSN: 2434-9186, 2434-9194. DOI: 10.35772/ghm.2021.01116. URL: https://www.jstage.jst.go.jp/article/ghm/4/3/4_2021.01116/_article.

[61] Kevin Zhang et al. "The impact of mask-wearing and shelter-in-place on COVID-19 outbreaks in the United States". In: *International Journal of Infectious Diseases* 101 (2020), pp. 334–341. ISSN: 12019712. DOI: 10.1016/j.ijid.2020.10.002. URL: https://linkinghub.elsevier.com/retrieve/pii/S1201971220322049.

[62] Ying Liu and Joacim Rocklöv. "The effective reproductive number of the Omicron variant of SARS-CoV-2 is several times relative to Delta". In: *Journal of Travel Medicine* 29.3 (31, 2022), taac037. ISSN: 1195-1982, 1708-8305. DOI: 10.1093/jtm/taac037. URL: https://academic.oup.com/jtm/article/doi/10.1093/jtm/taac037/6545354.

[63] Thomas N. Vilches et al. "Projecting the impact of a two-dose COVID-19 vaccination campaign in Ontario, Canada". In: *Vaccine* 39.17 (2021), pp. 2360–2365. ISSN: 0264410X. DOI: 10.1016/j.vaccine.2021.03.058. URL: https://linkinghub.elsevier.com/retrieve/pii/S0264410X21003625.

[64] Weijing Shang et al. "Percentage of Asymptomatic Infections among SARS-CoV-2 Omicron Variant-Positive Individuals: A Systematic Review and Meta-Analysis". In: *Vaccines* 10.7 (30, 2022), p. 1049. ISSN: 2076-393X. DOI: 10.3390/vaccines10071049. URL: https://www.mdpi.com/2076-393X/10/7/1049.

[65] Jantien A Backer et al. "Shorter serial intervals in SARS-CoV-2 cases with Omicron BA.1 variant compared with Delta variant, the Netherlands, 13 to 26 December 2021". In: *Eurosurveillance* 27.6 (10, 2022). ISSN: 1560-7917. DOI: 10.2807/1560-7917.ES.2022.27.6.2200042. URL: https://www.

eurosurveillance.org/content/10.2807/1560-7917.ES.2022.27.6.2200042.

[66] Mélanie Drolet et al. "Time trends in social contacts before and during the COVID-19 pandemic: the CONNECT study". In: *BMC Public Health* 22.1 (2022), p. 1032. ISSN: 1471-2458. DOI: 10.1186/s12889-022-13402-7. URL: https://bmcpublichealth.biomedcentral.com/articles/10.1186/s12889-022-13402-7.

[67] J.M Heffernan, R.J Smith, and L.M Wahl. "Perspectives on the basic reproductive ratio". In: *Journal of The Royal Society Interface* 2.4 (22, 2005), pp. 281–293. ISSN: 1742-5689, 1742-5662. DOI: 10.1098/rsif.2005.0042. URL: https://royalsocietypublishing.org/doi/10.1098/rsif.2005.0042.

[68] O. Diekmann, J. A. P. Heesterbeek, and M. G. Roberts. "The construction of next-generation matrices for compartmental epidemic models". In: *Journal of The Royal Society Interface* 7.47 (6, 2010), pp. 873–885. ISSN: 1742-5689, 1742-5662. DOI: 10.1098/rsif.2009.0386. URL: https://royalsocietypublishing.org/doi/10.1098/rsif.2009.0386.

[69] P. van den Driessche and James Watmough. "Reproduction numbers and sub-threshold endemic equilibria for compartmental models of disease transmission". In: *Mathematical Biosciences* 180.1 (2002), pp. 29–48. ISSN: 00255564. DOI: 10.1016/S0025-5564(02)00108-6. URL: https://linkinghub.elsevier.com/retrieve/pii/S0025556402001086.

[70] Tom Britton, Frank Ball, and Pieter Trapman. "A mathematical model reveals the influence of population heterogeneity on herd immunity to SARS-CoV-2". In: *Science* 369.6505 (14, 2020), pp. 846–849. ISSN: 0036-8075, 1095-9203. DOI: 10.1126/science.abc6810. URL: https://www.sciencemag.org/lookup/doi/10.1126/science.abc6810.

[71] Thomas J DiCiccio and Bradley Efron. "Bootstrap Confidence Intervals". In: ().

[72] Mark Stevenson et al. *epiR: Tools for the Analysis of Epidemiological Data*. 2023. URL: https://CRAN.R-project.org/package=epiR.

[73] Bertrand Iooss et al. *sensitivity: Global Sensitivity Analysis of Model Outputs*. 2022. URL: https://CRAN.R-project.org/package=sensitivity.

[74] M. Laskowski et al. "Strategies for Early Vaccination During Novel Influenza Outbreaks". In: *Scientific Reports* 5.1 (14, 2015), p. 18062. ISSN: 2045-2322. DOI: 10.1038/srep18062. URL: https://www.nature.com/articles/srep18062.

[75] Richard Taylor. "Interpretation of the Correlation Coefficient: A Basic Review". In: *Journal of Diagnostic Medical Sonography* 6.1 (1, 1990), pp. 35–39. ISSN: 8756-4793. DOI: 10.1177/875647939000600106. URL: https://doi.org/10.1177/875647939000600106.